Response to the Reviewers
Format: The reviewers' comments are quoted in italic
Section number in the response refers to the revised manuscript with tracked changes
Quotation in red stands for revised/added text in the revised manuscript

Overall comment:
We thank the reviewers for their detailed comments. The main revisions that we applied to the revised manuscript include: 1) examined whether aerosol measurements for Na_{500} are affected by the existence of ice particles at in-cloud conditions; 2) tested the impacts of using out-of-cloud Na_{500} variable to examine the correlations between Na_{500}, Na_{100}, and ice microphysical properties; 3) added more tests for the machine learning (ML) experiments to show the incremental value of adding individual predictors; and 4) examined the effects of using water vapor volume mixing ratio (q) as a predictor and compared with the effects of using RHi.

Below are our individual responses to the reviewers' comments and the corresponding changes.

Response to Reviewer 1's comments:

Ngo review

The authors evaluate relationships between cirrus microphysical properties and other relevant parameters using in situ observations from twelve field campaigns globally. The study focuses on comparing observations of microphysical properties with temperature, vertical air motion and aerosol concentrations using commonly deployed instrumentation. They perform multiple analyses - the two primary methodologies consist of comparisons of detrended datasets and another using a machine learning algorithm to determine how sufficiently the environmental parameters influence both the occurrence and properties of cirrus clouds.

The study addresses pressing questions concerning cirrus clouds, and figures throughout the manuscript were clear and well organized. However, I have a few major concerns which I discuss below. I also urge the authors to diligently proofread the manuscript, as many statements should be rewritten to improve clarity.

Major Concern #1:

It is common practice not to use aerosol measurements from spectrometers or CCN counters in cloud, but rather use measurements taken in clear-sky regions in the vicinity of the clouds of which they are compared to. This commonly involves obtaining measurements above or below cloud. I strongly suspect that Naer500 is sampling small ice particles, whether related to shattering or not, which is why such strong linear trends are observed in Figure 6 regardless of temperature, w, or RHi range.

It is crucial to show that measurements are not biased when using in-cloud measurements. Unfortunately, the large set of observations may make this a tedious task, but it is vital to assure these are accurate measurements as much of this manuscript evaluates aerosol-cloud interactions. I would recommend presenting multiple case studies from each campaign showing Naer500 in the vicinity of and within cloud.

Thank you for this comment. We took several approaches (described in more details below) to examine the possible artifact of Na_{500} measurements for in-cloud conditions by using case studies of time series for both NASA and NSF campaigns, as well as using a correlation analysis applied to Na_{500} and IWC. The results of these two analyses both showed that there are no second-to-second correlations between the fluctuations of Na_{500} and the fluctuations of IWC for in-cloud conditions. In fact, for most of the in-cloud samples (~70%), Na_{500} was reported to be zero (no large aerosols). In addition, we took another approach as suggested by the reviewer, to calculate Na_{500} at clear-sky regions that are adjacent to the in-cloud segments (using a moving average of 100 seconds). A similar linear regression figure using the clear-sky Na_{500} values shows very similar results to Figure 6 that uses the in-cloud Na_{500} values.

Regarding the reviewer's comment about whether aerosol measurements of Na_{500} are sampling small ice particles, it is quite unlikely since in this environment small ice crystals grow rapidly. When the UHSAS or FCAS only detect up to 1 μm, they would effectively be needing to capture the ice crystals immediately after nucleation in order to detect them, which we do not foresee happening. A modeling study by Jensen et al. (2024) also showed that the small ice particles (diameters < 10 μm but in particular less than 2 μm) are very transient and short-lived due to various effects after ice formation in cirrus clouds.

In a short summary, we added discussions of these additional analyses in the main text and added two supplemental figures (**Figures S6 and S7**). Because no evidence was found for the possible artifact of in-cloud Na_{500} measurements, we kept using the in-cloud Na_{500} variable as the main variable in the main manuscript, while also showing the sensitivity tests using the clear-sky Na_{500} variable in the supplemental material. Below we show the detailed response and the related table and figures for each approach mentioned in the overarching description above.

<u>Approach 1</u>. Examining potential artifacts of Na_{500} measurements for in-cloud conditions using case studies

Figure R1 below shows a time series of the NASA-DC3 campaign Research Flight (RF) 03, around UTC 25:40 to 26:00. Fluctuations of IWC are seen to be tightly correlated with Ni, as expected. However, the fluctuations of both Na_{100} and Na_{500} (last row) are found to be independent from those of IWC (first row). In fact, most of the 1-Hz in-cloud conditions are associated with Na_{500} values being zero. This indicates that the existence of ice particles is unlikely the cause of the higher Na_{500} values such as via small ice particle sublimation or large ice shattering. Because if that was the case, we would expect to see direct correlations between the fluctuations of the IWC and Na variables. Towards the end of this in-cloud period, Di decreases and Ni increases, but there are no measurements of Na_{500}. If there were to be a correlation between Na_{500} and small ice crystals, it should be when Di is smallest, which was not observed. In addition, since the existence of large aerosols ($Na_{500} > 0$) was observed less frequently compared with the existence of ice particles, this indicates that some of the ice particles are likely formed by homogeneous freezing. This also is consistent with the fact that ice nucleating particles (INPs) are very rare in the upper troposphere, and the existence of Na_{500} as a proxy of INP likely provides a significant support for ice nucleation by lowering the required energy barrier for heterogeneous freezing. We examined individual hourly segments of time series for all the campaigns used in this analysis. Here we only show one example, but no second-to-second correlation was found for other campaigns either.

We also investigate whether there are correlations between occurrences of large aerosols and a certain size range of ice particles. **Figure R2** shows the distribution of ice crystal number concentrations (Ni) and mean diameters (Di), showing in-cloud samples with or without $Na_{500} > 0$. The samples with large aerosols occur at various Ni and Di ranges, not only concentrated at either smaller or larger ice particles. This result indicates that there is no evidence showing that sublimation of small ice or shattering of large ice could be the main cause of large aerosol occurrences measured.

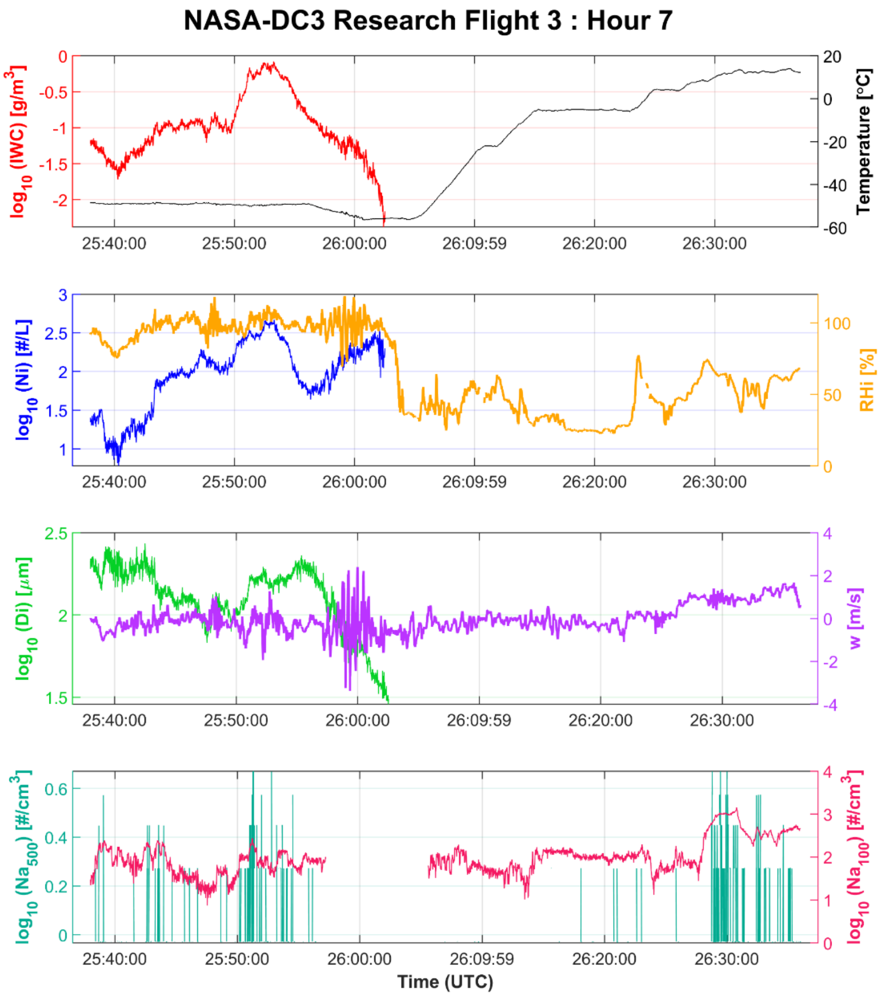

Figure R1. A case study of NASA DC-3 RF03 time series, illustrating the 1-Hz fluctuations of in-situ observations of ice microphysical properties (i.e., IWC, Ni and Di), aerosol number concentrations (Na_{100} and Na_{500}), and thermodynamic/dynamical variables (temperature, RHi, and w).

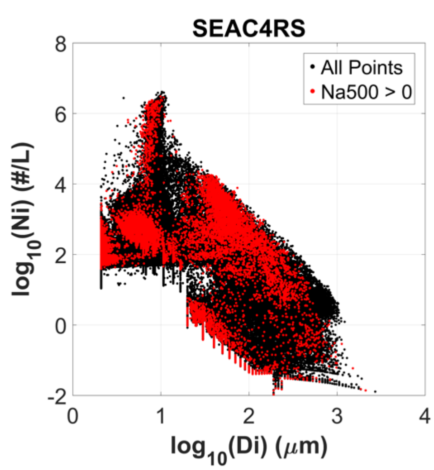

Figure R2. Correlations between Ni and Di in NASA SEAC[4]RS campaign, colored by the occurrences of Na_{500}. Black dots show all in-cloud samples (with or without Na_{500}), and red dots show in-cloud samples with $Na_{500} > 0$. All variables are plotted on a logarithmic scale.

Approach 2. Analyzing the number of samples for in-cloud or clear-sky conditions that also contain small and large aerosols to investigate possible correlations between Na_{500} and ice particles

Table R1 shows the number of samples for 4 scenarios, (1) in-cloud conditions with large aerosols (i.e., $Na_{500} > 0$), (2) in-cloud conditions with small aerosols ($Na_{100} > 0$), (3) clear-sky with large aerosols, and (4) clear-sky with small aerosols. The result shows that only 33 % of the in-cloud observations have $Na_{500} > 0$, indicating that the existence of ice particles does not always directly cause the occurrences of large aerosols.

In addition, **Table R2** uses a similar analysis to Table R1 except for adding a requirement of ice supersaturated conditions only (i.e., RHi > 100 %). After restricting each column to ice supersaturation (ISS) only, Table R2 shows that the ratios of number of samples between in-cloud and clear-sky conditions that are associated with both large aerosols and ISS are much higher than 1 (i.e., 6 – 16). Comparatively, without restricting to ISS only, Table R1 shows that the ratios are 0.006 – 0.7. This result shows that there is a higher fraction of in-cloud conditions for large aerosol samples when ISS is available. If ice sublimation or ice shattering is the main cause of large aerosols, one would not expect to see large aerosols occur more frequently when ISS is available. This feature suggests that the existence of both large aerosols and ISS is likely to cause ice nucleation to occur, instead of the other way around (e.g., ice crystals affecting aerosol measurements). It is possible that when large aerosols do not exist, ice particles may have been formed via homogeneous freezing. However, the small fraction of $Na_{500} > 0$ for in-cloud conditions cannot be interpreted as heterogeneous freezing having a smaller significance compared with homogeneous freezing, because once the ice crystals are formed, the INP particles will become part of ice and will exceed the size measurement range of the aerosol probe (60 nm – 1000 nm).

Table R1. The number of 1-second samples of four conditions, including in- or out-of-clouds, with or without the existence of various types of aerosols (i.e., Na_{500} or Na_{100} values being greater than zero).

# of 1-s observations in each temperature range	In-cloud & $Na_{500} > 0$	In-cloud & $Na_{100} > 0$	Clear sky & $Na_{500} > 0$	Clear sky & $Na_{100} > 0$
-50 < T ≤ -40°C	24026	90989	47658	374659
-60 < T ≤ -50°C	26847	82362	40005	358825
-70 < T ≤ -60°C	15755	27737	56543	167650
-80 < T ≤ -70°C	61	3531	10010	24197

Table R2. Similar to Table R1, except for analyzing ice supersaturated conditions only.

# of 1-s observations in each temperature range	In-cloud & $Na_{500} > 0$ & RHi > 100 %	In-cloud & $Na_{100} > 0$ & RHi > 100 %	Clear sky & $Na_{500} > 0$ & RHi > 100 %	Clear sky & $Na_{100} > 0$ & RHi > 100 %
-50 < T ≤ -40°C	8719	38587	1348	9848
-60 < T ≤ -50°C	7286	29233	1152	7505
-70 < T ≤ -60°C	4445	7603	332	2764
-80 < T ≤ -70°C	16	682	1	273

About the reviewer's comment about why the positive correlations between ice microphysical properties and Na_{500} and Na_{100} values can be seen for various T, RHi, and w ranges, we would like to clarify that the positive correlation at low RHi such as sub-saturated conditions may be caused by previous ice nucleation events happened before the aircraft sampling. That is, when the cirrus clouds were at the nucleation phase, some of the large aerosols likely acted as INPs and led to more ice particle formation, but later RHi decreased to sub-saturated conditions, and such correlations between ice microphysics and large aerosols could still be seen. Our previous study by Maciel et al. (2023) showed that the linear regression slope values are larger at nucleation phase and early growth phase, indicating stronger aerosol-cloud interactions (ACI) for those phases. The slopes decrease when cirrus clouds are in later growth and sedimentation phases, but it doesn't exclude the possibility that this positive correlation can still be seen after ice nucleation.

Approach 3. Conducting a sensitivity test that calculates average clear-sky Na_{500} for every 100 seconds and examining its correlations with ice microphysical properties.

The impacts of using aerosol measurements outside each in-cloud segment are also investigated. The out-of-cloud Na values were calculated for every 100-s and only the clear-sky segments out of the 100 seconds were used in the averaging. Correlations between the two types of Na values (in-cloud versus out-of-cloud) with respect to IWC values show very similar results. Correlation analyses in supplemental Figures S6 and S7 show consistent positive slope values with similar magnitudes compared with those shown in Figures 5 and 6, respectively. These results indicate that the positive correlations seen between IWC and Na are consistently found regardless using in-cloud aerosol measurements or the adjacent clear-sky aerosol measurements surrounding cloudy segments.

In summary, we added the comments regarding any possible aerosol measurement issues for in-cloud conditions in Section 2.1 "To examine if there are any possible artifacts in aerosol measurements for in-cloud conditions, we examined time series of 1-Hz measurements for IWC, Ni, Di, Na_{100}, and Na_{500} for various campaigns (not shown). No direct correlations were found between the cloud and aerosol measurements at cirrus regime at second-to-second resolution. Among all in-cloud samples, only 33 % contain large aerosols, while most in-cloud samples contain small aerosols, indicating that it is unlikely that the sublimation or shattering of ice crystals contributes to the existence of large aerosols (i.e., $Na_{500} > 0$). It is also unlikely that the aerosol measurements were detecting small ice crystals (a few microns), since the small ice crystals would grow rapidly. This speculation is also corroborated by a modeling study by Jensen et al. (2024), which showed that small ice particles (diameters < 10 μm but in particular less than 2 μm) are very transient and short-lived after ice formation in cirrus clouds.."

Reference mentioned above: Jensen, E. J., Kärcher, B., Woods, S., Krämer, M., and Ueyama, R.: The impact of gravity waves on the evolution of tropical anvil cirrus microphysical properties. Journal of Geophysical Research: Atmospheres, 129, e2023JD039887, https://doi.org/10.1029/2023JD039887, 2024.

We also added discussion in Section 3.3: "To further examine the role of aerosols in the ACI relationship, the number of samples of in-cloud and clear-sky conditions associated with large and small aerosols are analyzed. The results show that for large aerosol samples (i.e., $Na_{500} > 0$), 30 % of them are in-cloud while the rest are in clear-sky conditions. For small aerosol samples (i.e., $Na_{100} > 0$), 18 % of them are in-cloud. When restricted to ice supersaturated conditions only, a significant increase is seen for large aerosol samples associated with in-cloud conditions (75 %) while the rest are clear-sky conditions. Similarly, a significant increase is seen for small aerosol samples at in-cloud conditions (79 %) when ice supersaturation is available. In addition, when examining the distributions of Na_{500} at in-cloud conditions, the occurrences of large aerosols are seen at various Ni and Di ranges (not shown), suggesting that large aerosols are not solely observed when large or small ice crystals are available. These results suggest that it is more likely that the coexistence of aerosols and ice supersaturation leads to the formation of ice crystals instead of the other way around (i.e., occurrences of ice crystals affecting aerosol measurements)."

The investigation of clear-sky aerosols is also discussed in Section 3.3: "Even though no evidence was found regarding possible artifacts of in-cloud aerosol measurements as discussed in Section 2.1, we investigate the ACI relationships based on clear-sky aerosol number concentrations (Na) to further verify whether the observed ACI would still be seen when using coarser-scale Na for clear-sky conditions only. Specifically, for each center second, only the clear-sky segments of the surrounding 100 seconds are used for the calculation of clear-sky Na_{500} (or Na_{100}) values. In addition, at least 10 % of the 100 seconds have to be clear sky. If either of these two criteria is not satisfied, this second would be assigned NAN for the clear-sky Na value. Figure S6 shows similar positive relationships of IWC and Ni with respect to clear-sky Na_{500} and Na_{100} compared with Figure 5, indicating that the observed ACI relationships are consistently seen regardless of using aerosol information at finer or coarser resolution, in-cloud or clear-sky conditions. One main difference between Figure S6 and Figure 5 is that Figure S6 shows fewer Na with very high or low values, due to the averaging process for the clear-sky Na calculation. This averaging process may also lead to less significant increases of IWC, Ni, and Di with respect to Na_{100} in Figure S6, as the very high Na_{100} values are smoothed out."

Also, discussion is added to Section 3.4: "Similar to Section 3.3, clear-sky Na values are investigated for their correlations with ice microphysical properties. Linear regressions using clear-sky Na_{500} and Na_{100} are shown in Figure S7. Figure S7 shows similar positive correlations compared with Figure 6 for almost all IWC and Ni panels, except for the lowest temperature range for small aerosols (panels b1 and b2) possibly due to fewer samples. One main difference is that Figure S7 shows no clear trend for Di – Na relationships compared with Figure 6, which is likely due to the lack of high Na values as a result of the averaging process for clear-sky Na calculations."

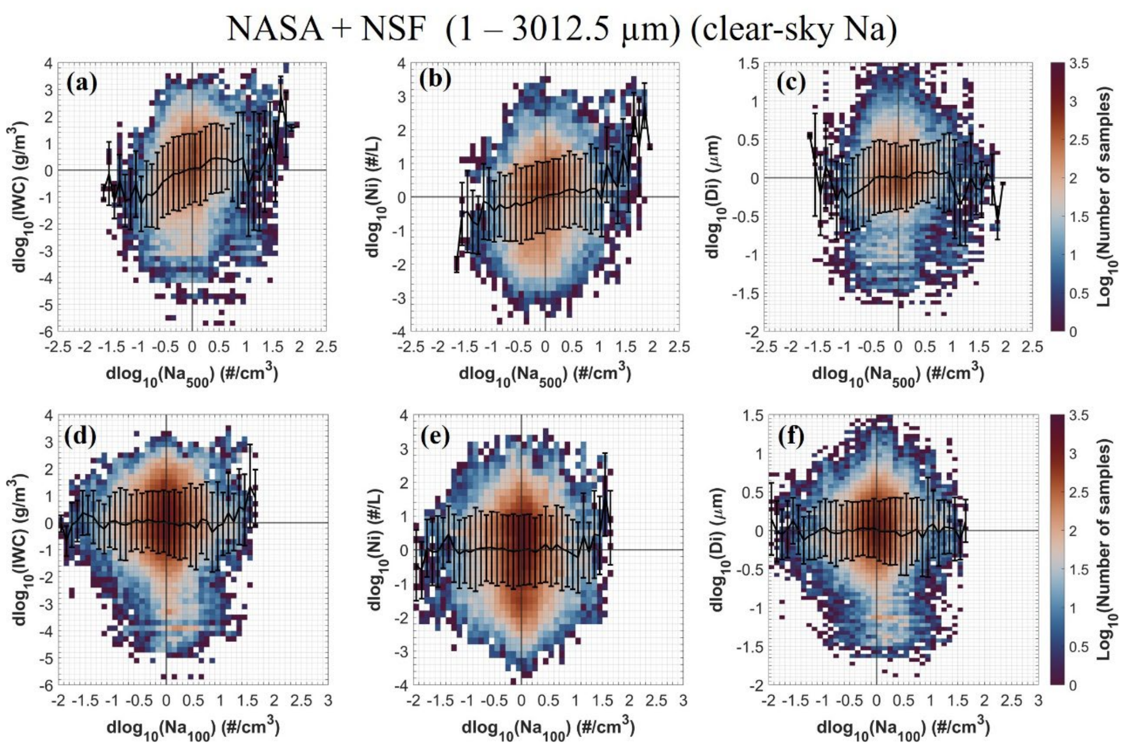

Figure S6. Similar to Figure 5, except for the analysis of clear-sky Na instead of in-cloud Na. Distributions of IWC, Ni, and Di with respect to (a-c) Na_{500} and (d-f) Na_{100} using the clear-sky Na values calculated at 100-s scale. Black lines and vertical bars denote the geometric means and standard deviations, respectively.

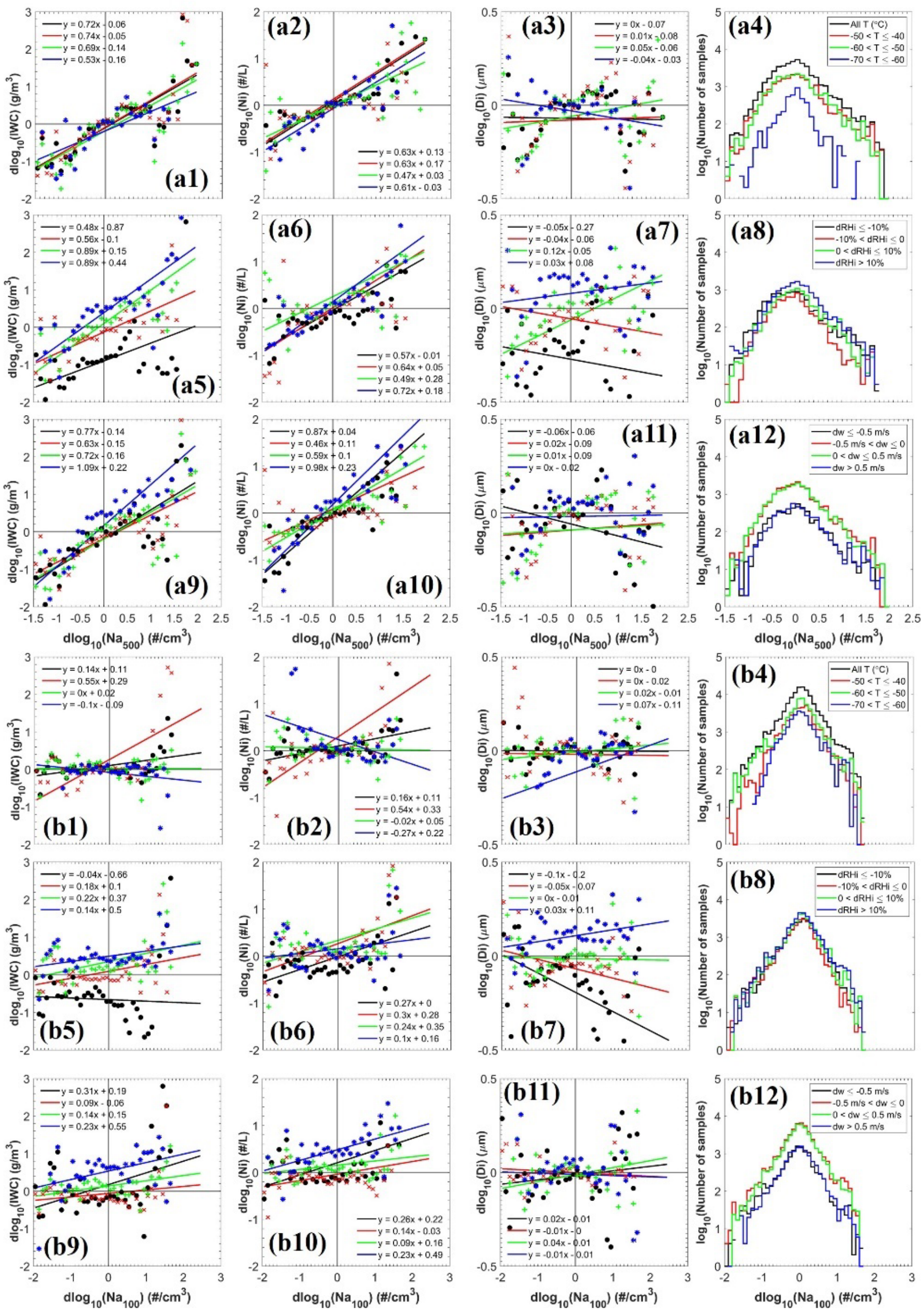

Figure S7. Similar to Figure 6 in the main manuscript, but using clear-sky Na values. ACI is examined for various ranges of temperature, dRHi, and d*w*. Colored dots represent geometric means of ice microphysical properties in each Na bin. Slope and intercept values are shown in the legend. The last column represents the number of samples.

Major Concern #2:

Perhaps not a major concern, but the in-cloud threshold is very low. Especially for OAP measurements that use particles down to diameters of 15 microns, this can result in in-cloud measurements below 10-7 g m-3, which is an extremely low and questionable threshold considering the relevance in columnar radiative fluxes. It would be prudent to test findings using a higher threshold, and at least provide sources as evidence for what in-cloud thresholds should be considered for thin cirrus which significantly impact radiative fluxes. I also mention this here as a major concern since I wouldn't expect the aerosol measurements to be biased at extremely low cloud thresholds, which should be taken into consideration when evaluating potential biases.

Thank you for this comment. We took two steps to address this comment. First, we added a discussion about the impact of IWC magnitude on cirrus optical depth and cloud radiative effects. Second, we conducted sensitivity tests to the linear regressions using different IWC thresholds for defining in-cloud conditions. In addition, we realized that we would benefit from a table showing measurement ranges of multiple variables. Thus, we added a new supplementary table at the end of Section 2.1.

Below is the new text added to the main manuscript:
"Table S2 shows the minimum and maximum range of several key variables for each campaign at cirrus cloud temperatures ≤ -40 °C. In this work we analyzed the entire range of IWC measurements including cirrus that may be subvisible for satellite retrievals. We also conducted sensitivity tests using higher IWC thresholds for in-cloud conditions (i.e., IWC > 10^{-5}, > 10^{-4}, and > 10^{-3} g m^{-3}) and the main ACI features were consistently found (to be discussed in Section 3.4). One should note that cirrus with different magnitudes of IWC has different radiative effects. Based on the previous work of Heymsfield et al. (2003), cirrus clouds with IWC of 10^{-7} and 10^{-5} g m^{-3} would have an optical depth of 3.3×10^{-5} and 0.0015, respectively, for a cirrus layer with 1-km thickness using the equation of $\tau = 0.069(IWP)^{0.83}$, where τ is optical depth and IWP is ice water path. In addition, calculations of a radiative transfer model showed that cirrus radiative effects in shortwave and longwave radiation become more noticeable (i.e., < -0.25 and > 0.25 W m^{-2}, respectively) when the cloud optical depth is larger than 0.001 (Spang et al., 2024)."

References mentioned above:

Heymsfield, A. J., Matrosov, S., and Baum, B.: Ice Water Path–Optical Depth Relationships for Cirrus and Deep Stratiform Ice Cloud Layers. J. Appl. Meteor. Climatol., 42, 1369–1390, https://doi.org/10.1175/1520-0450(2003)042<1369:IWPDRF>2.0.CO;2, 2003.

Spang, R., Müller, R., and Rap, A.: Radiative effect of thin cirrus clouds in the extratropical lowermost stratosphere and tropopause region, Atmos. Chem. Phys., 24, 1213–1230, https://doi.org/10.5194/acp-24-1213-2024, 2024.

In addition, we added discussion in Section 3.4: "A sensitivity test is also conducted using various IWC thresholds to define in-cloud conditions, i.e., IWC > 10^{-5} g m^{-3}, > 10^{-4} g m^{-3}, or > 10^{-3} g m^{-3} in Figures S8 – S10, respectively. The slope values of the linear regressions show almost all positive values for the correlations of IWC, Ni, and Di with respect to Na_{500} and Na_{100}, except for the lowest temperature range (-70° to -60°C in panel b2 of Figures S9 and S10) where negative correlations between Na_{100} and Ni are seen. This exception is likely caused by higher IWC thresholds significantly reducing the in-cloud sample size, as seen in the last column of those figures."

Table S2. The measurement range (minimum; maximum) of several key variables for individual campaigns restricted to cirrus cloud temperatures ≤ -40 °C.

Campaign	**T (°C)**	**P (hPa)**	**RHi (%)**	**IWC (g/m^3)**	**Ni (#/L)**	**Di (μm)**	**Na_{500} ($\#/cm^3$)**	**Na_{100} ($\#/cm^3$)**
ATTREX	-88.1; -40	68.1; 330.5	1.65; 206.1	4.41×10^{-8}; 0.443	0.037; 2.14×10^{4}	2.25; 401.32	-	-
POSIDON	-87.8; -40	63.1; 252.9	5.50; 212.4	7.68×10^{-8}; 1.61	0.041; 2.26×10^{4}	2.25; 1510	-	-
SEAC^{4}RS	-59.5; -40	178.7; 289.8	2.06; 156.7	4.86×10^{-8}; 3.30	0.010; 3.10×10^{4}	2.10; 1455	0; 69.3	0; 688.4
NASA-DC3	-63.5; -40	178.2; 297.5	1.54; 161.8	3.19×10^{-6}; 3.68	0.009; 1.70×10^{5}	20.0; 2500	0; 61.0	0; 3.55×10^{3}
MACPEX	-77.5; -40	74.1; 347.1	1.80; 161.8	2.73×10^{-6}; 0.528	0.019; 1.95×10^{3}	20.0; 2105	0; 449.0	0; 2.10×10^{3}
CONTRAST	-78.3; -40	126.6; 331.3	0.378; 177.3	1.27×10^{-7}; 1.02	0.042; 7.05×10^{3}	2.50; 1575	0; 6.86	0; 2.91×10^{3}
NSF-DC3	-65.8; -40	146.7; 321.9	1.24; 161.2	1.22×10^{-7}; 1.44	0.046; 1.81×10^{5}	2.50; 2150	0; 15.2	0; 1.53×10^{3}
HIPPO	-77.2; -40	132.8; 531.3	0.482; 174.9	1.27×10^{-7}; 0.930	0.042; 1.61×10^{4}	2.50; 2950	0; 712.2	0; 7.88×10^{3}
ORCAS	-68.8; -40	176.3; 433.2	0.334; 171.7	1.08×10^{-7}; 0.243	0.043; 5.22×10^{3}	2.50; 975	0; 60.5	0; 537.2
PREDICT	-71.4; -40	140.3; 273.3	0.635; 191.7	1.27×10^{-7}; 1.58	0.043; 4.06×10^{4}	2.50; 2850	0; 84.5	0; 568.6
START08	-67.6; -40	132.8; 447.3	0.331; 143.4	1.27×10^{-7}; 1.68	0.042; 6.08×10^{3}	2.50; 1600	-	-
TORERO	-74.9; -40	123.8; 345.3	0.665; 149.6	4.29×10^{-8}; 0.521	0.046; 1.37×10^{3}	2.50; 2200	0; 6.07	0; 274.13

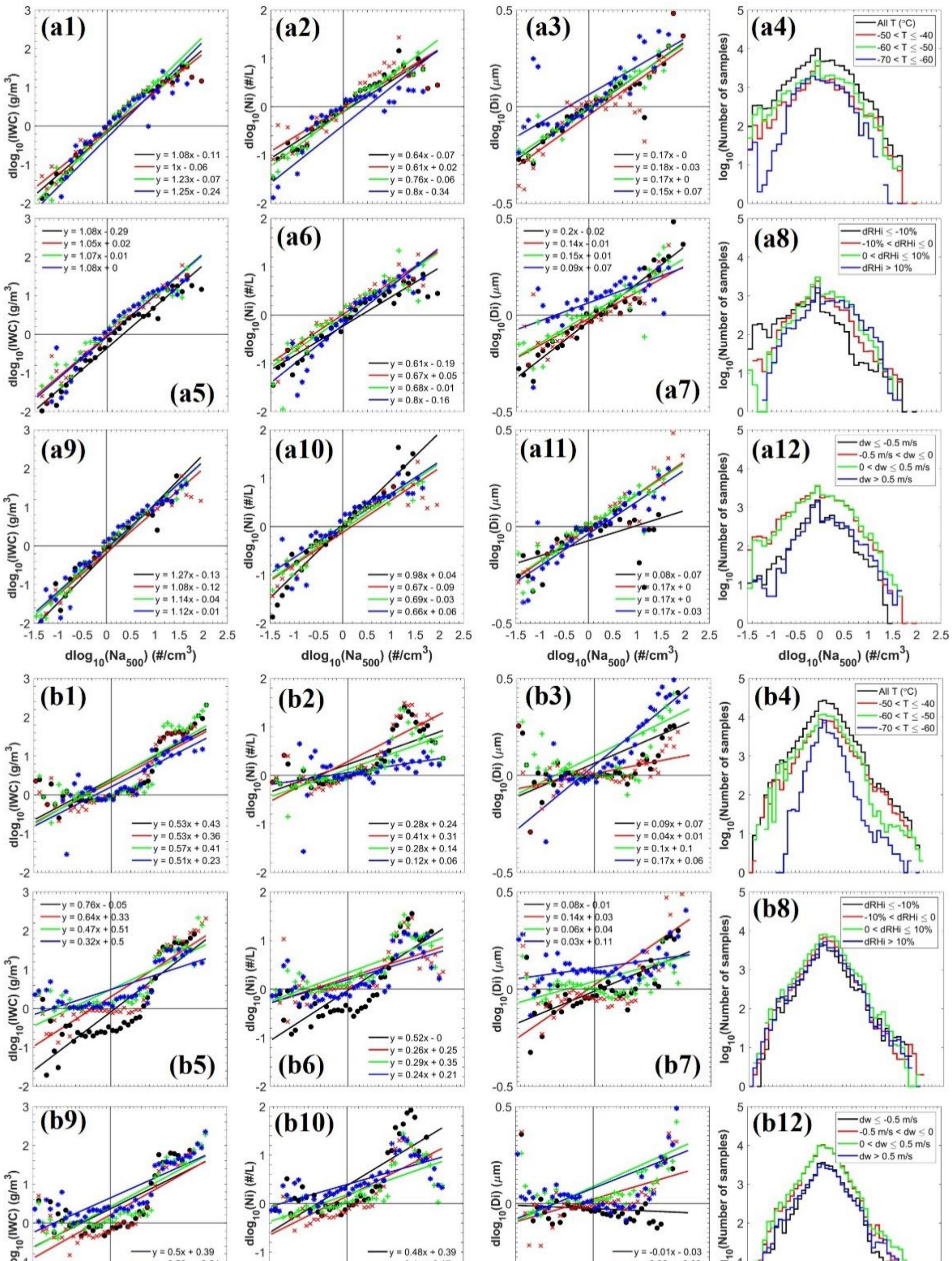

Figure S8. Similar to Figure 6 in the main manuscript, except for using a higher threshold for in-cloud definition, i.e., in-cloud conditions are defined as IWC > 10^{-5} g m^{-3}.

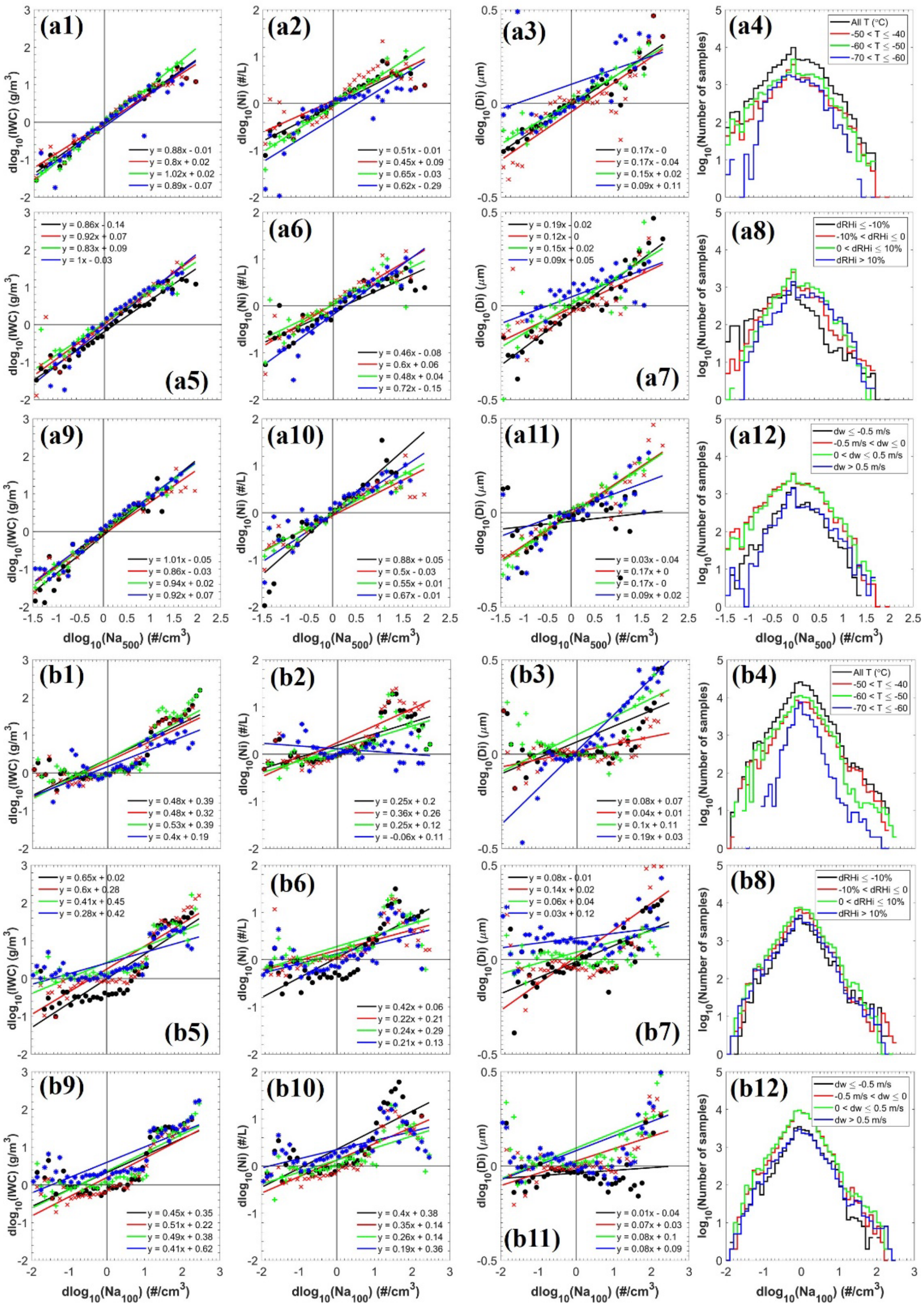

Figure S9. Similar to Figure 6 in the main manuscript, except for using a higher threshold for in-cloud definition, i.e., in-cloud conditions are defined as IWC > 10^{-4} g m^{-3}.

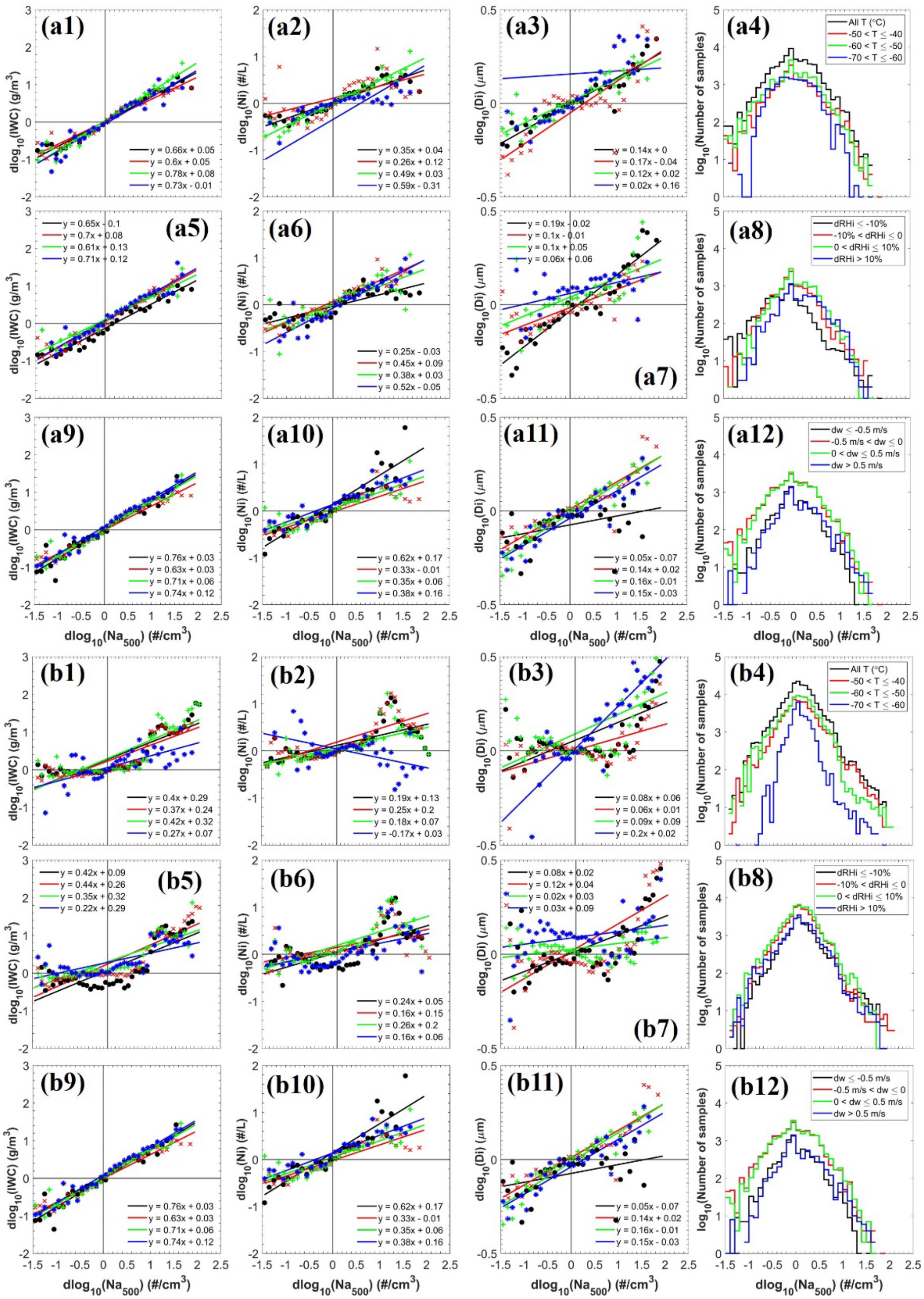

Figure S10. Similar to Figure 6 in the main manuscript, except for using a higher threshold for in-cloud definition, i.e., in-cloud conditions are defined as IWC > 10^{-3} g m^{-3}.

Major Concern #3:

I worry the machine learning methodology is not sound. It seems the authors are using it to discern which environmental parameters cirrus cloud occurrence frequencies and microphysical properties are most sensitive to. However, they only use a select few combinations of predictor variables when evaluating the success rate of the model to simulate the observations for Test B and C. Due to the "black box" nature of the ML method, we need to test all possible combinations of the predictor variables and weight their success rates accordingly.

The authors qualitatively do this for Test A in Table 2, but they don't explicitly state the importance of evaluating all possible combinations of predictor variables. They also don't provide any quantitative weighting measure of all possible predictor combinations. For example, they state for Test A that RHi is the most important predictor for the presence of cirrus (line 484-485). However, an argument could be made that Naer500 is just as important considering the approximately similar successful prediction rates of RHi and Naer500 as single variable predictors for all cirrus.

The methodology also does not account for the fact that RHi is intimately related to w and T. Thus, RHi inherently contains a signal of T and w within its calculation, and the findings actually state something along the lines of "water vapor and T is a better predictor than T", which is to be expected. It would benefit greatly to compare parameters which are completely independent of each other (e.g., aerosols vs RHi+w+T or water vapor vs T).

We thank you for this helpful comment. The reviewer mentioned that the original ML analyses did not clearly weigh the importance of adding each predictor variable. To address this issue, we revised our analysis to include all possible combinations of predictors in the revised **Table 2**. This includes a total of 31 sets of combinations. In the previous analysis of the original manuscript, the ML tests using only T, RH, and w (i.e., without aerosol information) were based on all 12 campaigns (including 7 NSF and 5 NASA campaigns), while the ML tests using aerosols as predictors excluded ATTREX, POSIDON, and START08 campaigns since they didn't have aerosol measurements. In the revised manuscript, in order to make each set of predictors more comparable to each other, we had to revise all the ML experiments to use the same set of data for all the combinations in Tests A, B and C. That is, all ML tests in the revised Tables 2 and 3 as well as Figures 7 – 10 now exclude ATTREX, POSIDON, and START08. This is because if we do not exclude these campaigns, the ML tests would use different sets of training and testing data, and the comparison results are not directly comparable. We also compared the new results to the original results, and the differences are minimal. We moved the original Table 2 into the supplementary **Table S4**, which includes the three additional campaigns (i.e., ATTREX, POSIDON, and START08) for tests using T, RH and *w* predictors only. We also clarified which datasets are being used in each figure and table here: "The NSF START08, NASA ATTREX, and NASA POSIDON campaigns were not included in the analysis of ACI due to the lack of aerosol measurements. Thus, these campaigns were excluded from the analysis used in Figures 5 – 10 as well as Tables 2 and 3."

After using the same dataset for all predictors, the single predictor RHi shows an even higher accuracy of 91% compared with the single predictor Na_{500} (84%). In addition, when combining with the T predictor, the T+RHi shows 92%, and the T+Na_{500} shows 73%. This reduction of accuracy for T+Na_{500} is likely caused by a common issue of ML experiments, i.e., when adding more predictors that are less correlated with the resultant variable, the additional predictors will cause noise amplification to the ML model and reduce the prediction accuracy compared with using key predictors only. To put this in a more straightforward perspective, the Na_{500} variable has a large number of samples equal to 0. When only using the Na_{500} as a predictor, the ML model learns to predict whether the condition is in or out of clouds using just the non-zero Na_{500} values. However, when T is added, a large amount of samples having real T values but no Na_{500} values, then the ML model needs to learn how to predict in or out of clouds just relying on T only. This will lower the accuracy of the entire prediction since T by itself is not a good predictor. Note that in our former response to main comment #1, we already demonstrated that there is no second-to-second correlation between Na_{500} and ice microphysical properties and no indications of measurement artifacts were found. The Na_{500} variable is likely a good predictor of in-cloud conditions because of larger aerosols serving as effective INPs.

On the other hand, when we look at the single RHi predictor (91% accuracy) compared with T+RHi (92% accuracy), their accuracies are very similar, indicating the RHi is consistently a highly effective predictor for predicting in-cloud conditions. We also applied a test to the T+RHi prediction by setting all RHi < 100% as zeros. This new T+RHi test shows an accuracy of 86% for all cirrus, which is lower than using RHi only (91%). This test further verifies our speculation above that using T+Na_{500} together reduces the accuracy of prediction compared with using Na_{500} only, because T introduces more noise into the prediction when there are many samples with zero Na_{500}.

Regarding the reviewer's comments about showing all sets of combinations for Test B (Table 3, Figures 8) and Test C (Figures 9 and 10) to provide more direct comparisons between predictors, we made the following changes: (1) All predictions in the revised Table 3 now use 9 flight campaigns by excluding ATTREX, POSIDON and START08 to make these predictions more comparable with each other; and (2) Two more rows were added to Figure 10 to show aerosol influences by using T+RHi+*w*+Na_{500}+Na_{100} to contrast with T+RHi+*w*. Note that we did not repeat all 31 sets of predictor combinations for Table 3 and Figures 8 – 10 as we did in Table 2, because of two main reasons. The first reason is that from the discussion right above this paragraph, we found that tests using a single variable predictor of aerosols (Na_{500} and Na_{100}) cannot provide a fair comparison with those using a single indicator of other variables (T, RHi, and *w*), because there are so many more zeros in aerosol measurements. Instead, we found that analyzing the incremental value of adding aerosol variables to the combination of T+RHi+w can better show the value of representing aerosols correctly for model parameterization purposes. The second main reason is for the clarity of display of these table and figures. Table 3 focuses on contrasting 5 different spatial scales, and if we show 31 sets of combinations at each scale, that will lead to 155 rows. Similarly, Figure 9 will need 31 rows and 93 panels, and Figure 10 will need 62 rows and 186 panels if one shows all combinations. Because Test A in Table 2 already demonstrated the importance of several key sets of combinations, we focus on those key combinations to reduce data cluster.

Regarding the reviewer's comment about testing water vapor instead of RHi as a predictor, we also ran a new series of ML tests for all combinations by replacing RHi with q (water vapor volume mixing ratio with a unit of ppmv). We added this result as **Table S5** in the supplementary file. The results showed that only using q has 76% accuracy, while using T+q has 91% accuracy (i.e., very similar to the accuracy of 91% by only using the RHi predictor). This result indicates that the RHi variable carries information for both T and q when predicting in-cloud conditions. However, we decided to use RHi as the default predictor in the main manuscript and kept this new q predictor table in the supplementary material, because RHi is often used as a parameter in global climate model (GCM) parameterizations for ice cloud macro- and microphysical properties (e.g., Gettelman and Kinnison, 2007; Tompkin et al., 2007). Thus, the ML results here can provide quantitative information for evaluating GCM simulations. Another reason for keeping RHi in the analysis of the main manuscript is that one may argue that almost all these five predictors are intertwined with each other, between T, RHi, w, Na_{500}, and Na_{100}. For instance, higher T is usually associated with higher Na values, while updraft (w > 0) can lead to cooling of the parcel (lower T and higher RHi). Because all these variables are not completely independent, we kept using RHi for its more common usage in model parameterizations.

We summarized this new result and added the text to the revised manuscript: "For this section, all the ML-based analysis uses the combined NASA+NSF dataset, but NSF START08, NASA ATTREX, and NASA POSIDON campaigns are not included due to the lack of aerosol measurements. A similar sensitivity test that includes these three campaigns for T, RHi, and *w* predictors is shown in supplemental Table S4. Similar results are seen compared with those in Table 2. All the tests that include RHi as a predictor have consistently high accuracies exceeding 91 %, which show that RHi is consistently the most important factor among all five variables. … Using Na_{500} as a single predictor also shows high accuracy of 84 % for all cirrus, but the accuracy decreases to 72 % when using T+Na_{500}. This is likely because when using only Na_{500}, the ML model focuses on a small number of samples with non-zero values of Na_{500} for predicting in-cloud conditions, while adding T predictor can lead to noise amplification as the ML model would need to predict cirrus occurrences using many T samples without Na_{500} information (i.e., Na_{500} = 0). To further verify if the effect of RHi ultimately represents influences from both water vapor volume mixing ratio (q) and temperature, another series of ML tests similar to Test A were conducted by using q as the predictor (supplemental Table S5). The result shows that having q as the single predictor has lower accuracy (76 %) than RHi (91 %), while using T+q has a similar accuracy (91 %) to RHi. Because of the frequent usage of RHi in model parameterizations of ice cloud macro- and microphysical properties (e.g., Gettelman and Kinnison, 2007; Tompkins et al., 2007), RHi is used for the rest of the ML analyses in the main manuscript."

References mentioned above:

Gettelman, A. and Kinnison, D. E.: The global impact of supersaturation in a coupled chemistry-climate model, Atmos. Chem. Phys., 7, 1629–1643, https://doi.org/10.5194/acp-7-1629-2007, 2007.

Tompkins, A. M., Gierens, K., and Rädel, G.: Ice supersaturation in the ECMWF integrated forecast system, Q J R Meteorol Soc, 133, 53–63, 2007.

Table 2. Summary of results for Test A, namely predicting the occurrences of cirrus clouds. Accuracies of the predictions are shown for all cirrus, vertically quiescent, and non-quiescent cirrus in columns 1 – 3, respectively. All possible combinations among five predictors are shown.

Predictors	***Accuracy (%) All cirrus***	***Accuracy (%) Vertically quiescent cirrus***	***Accuracy (%) Non-quiescent cirrus***
1 Predictor			
T	63.57	65.70	54.63
RHi	91.33	91.86	89.07
w	71.06	75.98	50.34
Na_{500}	84.17	88.81	64.68
Na_{100}	69.02	70.35	63.42
2 Predictors			
$T + RHi$	91.55	92.14	89.04
$T + w$	73.18	77.93	53.19
$T + Na_{500}$	71.92	74.74	60.06
$T + Na_{100}$	68.94	70.28	63.30
$RHi + w$	91.33	91.86	89.07
$RHi + Na_{500}$	91.35	91.90	89.04
$RHi + Na_{100}$	91.51	92.09	89.04
$w + Na_{500}$	76.16	81.40	54.11
$w + Na_{100}$	70.69	73.73	57.93
$Na_{500} + Na_{100}$	72.46	74.05	65.78
3 Predictors			
$T + RHi + w$	91.90	92.57	89.09
$T + RHi + Na_{500}$	91.89	92.55	89.10
$T + RHi + Na_{100}$	91.72	92.31	89.23
$T + w + Na_{500}$	77.69	82.75	56.40
$T + w + Na_{100}$	74.46	77.33	62.35
$T + Na_{500} + Na_{100}$	71.68	73.70	63.21
$RHi + Na_{500} + Na_{100}$	91.64	92.24	89.11
$RHi + w + Na_{500}$	91.56	92.16	89.07
$RHi + w + Na_{100}$	91.60	92.23	88.94
$w + Na_{500} + Na_{100}$	74.89	78.55	59.52
4 Predictors			
$T + RHi + w + Na_{500}$	91.96	92.66	89.00
$T + RHi + w + Na_{100}$	91.86	92.51	89.14
$T + RHi + Na_{500} + Na_{100}$	91.80	92.42	89.18
$T + w + Na_{500} + Na_{100}$	76.74	79.87	63.59
$RHi + w + Na_{500} + Na_{100}$	91.74	92.37	89.09
5 Predictors			
$T + RHi + w + Na_{500} + Na_{100}$	92.06	92.74	89.20

Table S4. Similar to Table 2 in Test A, but instead of excluding ATTREX, POSIDON, and START08 due to the lack of aerosol measurements, this Table S4 uses all NASA and NSF campaigns for ML experiments involved with predictors of T, RHi, and *w*. Accuracies of the cirrus occurrence predictions are shown for all cirrus, vertically quiescent, and non-quiescent cirrus in columns 1 – 3, respectively.

Predictors	***Accuracy (%) All cirrus***	***Accuracy (%) Vertically quiescent cirrus***	***Accuracy (%) Non-quiescent cirrus***
1 Predictor			
T	57.30	57.69	55.32
RHi	85.30	85.01	86.79
w	68.04	71.39	50.79
2 Predictors			
T + RHi	86.53	86.41	87.16
T + w	64.18	66.39	52.80
RHi + w	85.41	85.16	86.73
3 Predictors			
T + RHi + w	86.58	86.46	87.20

Table S5. Similar to Table 2, except using water vapor volume mixing ratio "q" (unit: ppmv) instead of RHi.

Predictors	***Accuracy (%) All cirrus***	***Accuracy (%) Vertically quiescent cirrus***	***Accuracy (%) Non-quiescent cirrus***
1 Predictor			
T	63.46	65.65	54.26
q	76.38	76.41	76.25
w	71.04	75.96	50.37
Na_{500}	84.32	88.96	64.83
Na_{100}	68.94	70.27	63.33
2 Predictors			
$T + q$	90.59	90.89	89.35
$T + w$	73.23	78.02	53.07
$T + Na_{500}$	73.18	76.18	60.55
$T + Na_{100}$	68.70	69.98	63.30
$q + w$	76.40	76.46	76.12
$q + Na_{500}$	77.23	77.02	78.13
$q + Na_{100}$	79.83	80.31	77.82
$w + Na_{500}$	76.17	81.42	54.11
$w + Na_{100}$	70.78	73.85	57.87
$Na_{500} + Na_{100}$	72.63	74.24	65.86
3 Predictors			
$T + q + w$	90.31	90.63	88.99
$T + q + Na_{500}$	90.76	91.12	89.23
$T + q + Na_{100}$	90.92	91.33	89.18
$T + w + Na_{500}$	77.50	82.51	56.45
$T + w + Na_{100}$	74.23	77.10	62.18
$T + Na_{500} + Na_{100}$	71.55	73.49	63.40
$q + Na_{500} + Na_{100}$	80.47	80.85	78.89
$q + w + Na_{500}$	77.17	76.93	78.19
$q + w + Na_{100}$	80.04	80.27	79.07
$w + Na_{500} + Na_{100}$	74.83	78.51	59.37

4 Predictors			
$T + q + w + Na_{500}$	90.47	90.79	89.12
$T + q + w + Na_{100}$	90.52	90.90	88.96
$T + q + Na_{500} + Na_{100}$	90.90	91.33	89.09
$T + w + Na_{500} + Na_{100}$	76.66	79.84	63.27
$q + w + Na_{500} + Na_{100}$	80.94	81.07	80.40
5 Predictors			
$T + q + w + Na_{500} + Na_{100}$	90.58	90.97	88.98

Additional comments:

Line 16: "with stronger AIE from larger aerosols than smaller ones" this doesn't make sense, please rephrase

We revised to: "Positive correlations were found between the fluctuations of these ice microphysical properties and the fluctuations of aerosol number concentrations for larger (> 500 nm) and smaller (> 100 nm) aerosols (i.e., Na_{500} and Na_{100}, respectively). Steeper linear regression slopes were seen for large aerosols compared with smaller aerosols."

Line 25: "Cirrus clouds are one…surface of 20%"

This sentence has been revised and more information has been added: "Cirrus clouds are the one of the most prominent cloud types with a wide spatial coverage over the Earth's surface. … The global cirrus coverage was reported to range from 10 % to 30 % from the polar regions to the tropics, respectively, based on observations of the Cloud-Aerosol Lidar and Infrared Pathfinder Satellite Observations (CALIPSO) satellite (Sassen et al., 2008 in their Figure 2). Wang et al. (2024) showed cirrus frequency around 20 % – 25 % at various latitudes and longitudes (in their Figure S6) based on several satellite products (e.g., CALIPSO and CloudSat)."

Line 28-30: Source?

We added more references to this part: "Because of the unique features of cirrus clouds, such as their thin, patchy nature (e.g., Sassen and Campbell, 2001), high altitudes (e.g., Lynch et al., 2002), complex ice morphology (e.g., Schnaiter et al., 2012), and the large spatial heterogeneities of their macro- and microphysical properties (e.g., Diao et al., 2014a, b; Maciel et al., 2023) ..."

Line 35-37: You're not using radiative effect correctly. Should change to flux.

Revised.

Line 42-44: It seems findings suggest that either pore condensation freezing or depositional nucleation is occurring at very high rates in the upper troposphere given the strong relationships to Naer500 and cirrus properties. It would be helpful to circle back to this occasionally in the paper. I found myself wondering "why are we looking for ice nucleation signatures at temperatures where ice will instantaneously freeze?" while reading this paper. It seems this would be the reason why.

We would like to clarify that the instantaneous ice freezing that the reviewer mentioned at the low temperatures analyzed here (i.e., ≤ -40°C) is related to freezing of liquid droplets, not the freezing of liquid aerosols or nucleation/freezing involving ice nucleating particles (INPs): "Even though liquid droplets can freeze instantaneously at these low temperatures, ice nucleation involving liquid aerosols and solid particles still requires relatively higher ice supersaturation (e.g., > 20 %)."

Line 44: The use of aerosol indirect effect is misleading in this paper. The term refers to how aerosols alter cloud properties by directly impacting cloud particle characteristics, which in turn feedback towards impacting radiative fluxes, precipitation initiation, etc. I'd recommend rewriting the paper and interchanging AIE with aerosol-cloud interactions or something comparable.

We revised the term to "aerosol-cloud interactions" for various locations across the manuscript. The title of the manuscript is also revised to: "Aerosol-Cloud Interactions in Cirrus Clouds Based on Global-Scale Airborne Observations and Machine Learning Models"

Line 51: 0<T<38C

Revised.

Line 70: "allow for a"

Revised.

Line 115: Perhaps reference the maps in the supplementary material only showing flight paths at T<-40C here.

We revised this part as the reviewer suggested by adding references to the flight track maps at low temperatures: "Global maps illustrating the entire flight tracks at all temperatures are shown for individual NASA and NSF campaigns in Figure 1. Flight tracks restricted to cirrus temperatures (≤ -40°C) are illustrated in supplementary Figures S1 and S2 for in-cloud and clear-sky conditions, respectively."

Line 156: "were taken from the"

Revised.

Line 165: "diameter" not "dynamic"

Revised.

Line 187-188: Rewrite this so the brown and francis 1995 study is referring only OAP measurements.

We added more information to this part: "IWC was derived based on the mass-dimensional relationship following Brown and Francis (1995) for Fast-2DC, CDP, FCDP, and Hawkeye-FCDP. For the 2D-S probe, the archived IWC data in each NASA campaign were used, which are based on the parameterizations from Baker and Lawson (2006). Because the parameterizations in Baker and Lawson (2006) require additional information besides the maximum dimension, such as width, area, perimeter, and categories of ice morphology, they were not applied to the other optical array probes."

Line 192: Rewrite this so it states what is being shown in the supplementary material not in the following sentence.

Revised.

Line 201: Here and Line 280, you say the "delta-delta" method remove the "temperature effect". What does this mean? Shouldn't this be rephrased to say something along the lines of "detrending the data in relation to variable X"?

We would like to clarify that the delta-delta method is not the same as conventional detrending along time series, since detrending usually means calculating the mean value for a continuous section of time series, and then calculating the differences between each second and that mean value. The delta-delta method calculates the mean value for each temperature bin (here binned by 1 degree Celsius), and then calculates the differences between each second within that temperature bin and that mean value of the bin. So the delta-delta method removes the trend of a variable as a function of temperature.

We clarified this part in the text: "In the previous studies of Patnaude and Diao (2020) and Maciel et al. (2023), a "delta-delta" method was developed to individually examine the thermodynamic/dynamic effects and aerosol effects on cirrus microphysical properties. This method calculates the mean value for each temperature bin (e.g., binned by 1 °C), and then calculates the differences between each 1-s variable value within that temperature bin and the mean value of the temperature bin. Thus, the delta-delta method removes the trend of a variable as a function of temperature. Note that the delta-delta method is different from detrending the data by subtracting the averaged values from each 1-Hz data along time series. After applying the delta-delta method, linear regressions can be applied to quantify the correlations between fluctuations of a certain environmental factor and the fluctuations of a cirrus microphysical property. However, one limitation of such analysis is the difficulty of conducting a direct, quantitative comparison among multiple factors. Thus, to achieve a direct comparison of multiple factors, an ML approach was developed in this work."

Line 205-206: Rephrase this sentence.

We rephrased this section: "To develop "training" and "testing" datasets for the ML models, the entire observation data of each research flight were first separated into 10 consecutive flight segments."

Section 2.2 seems out of place, and was confusing without giving a clear understanding of what machine learning will be used for. The objectives should be stated more clearly, and how the ML method specifically addresses them.

We can see why the original section on ML model description seems out of place. We revised this Section 2.2 to cover both methods: "2.2 Methods used to quantify influences of multiple factors on ice microphysical properties", including two sub-sections on the delta-delta method and the ML model method. In addition, we added more explanations of the objectives of the ML model to the beginning of Section 2.2.2, so the scientific goal is more clearly described early on: "ML models were developed to examine the influences of various factors through direct comparisons of the model prediction results. By using different combinations of predictors, prediction accuracies can be used to show the incremental values of individual variables."

Line 234-237: This was confusing, until thinking about it you meant that quiescent conditions correspond to convective and non-quiescent correspond to in situ, yes? Either way, specifically state and argue for why your conditions are comparable to those from Kramer.

We can see why the two definitions look similar and could have some overlapping samples. However, we also added text to clarify that we cannot provide a one-to-one comparison with Krämer's definition of convective clouds: "For instance, the high vertical velocity condition defined as non-quiescent in this work may indicate convective influences, but may also be caused by other dynamic conditions such as gravity waves and strong turbulence. Thus, we did not attempt to provide a one-to-one comparison between the non-quiescent condition in this work and the convective (liquid-origin) cirrus in the previous work by Krämer et al. (2016, 2020).”

Line 251-253: 1) I think you mean Figure 2.

Revised.

Line 229 & Line 260: These two range of +/- 30 seconds and 10 km, what is the rationale for selecting these lengths?

We added more discussion on the spatial scale: “A previous study of Diao et al. (2014a) analyzed the horiziontal length distributions of ice supersaturated regions (ISSRs), which are the prerequisite condition of cirrus clouds. That study showed that ~5% of the ISSR samples (i.e., one consecutive ISSR counted as one sample) exceed the 10 km horizontal scale while most ISSRs are relatively small, indicating that they are significantly affected by microscale dynamics but can also be affected by mesoscale dynamics. Therefore, the spatial window of ± 30 seconds (i.e., ~12 km horizontal scale) was chosen in this work to categorize two dynamic conditions.”

Line 281-283: How?

We added more clarification here: “As described in Section 2.2.1, the delta value is calculated by subtracting the average value of a certain variable in each 1 °C temperature bin from every 1-second datum, which removes the average increasing or decreasing trend of a variable as a function of temperature.”

Line 288-290: How do we know it’s sustained? I’d change “indicating” to “suggests”

We revised this part: “For example, both NASA and NSF datasets show a peak of $d\log_{10}$IWC and $d\log_{10}$Ni at dRHi slightly above 0 % (i.e., dRHi of 10 % – 20 %). This result is consistent with that seen in Patnaude and Diao (2020), suggesting that the highest IWC and Ni may be reached shortly before all the ice supersaturation has been depleted through new ice particle formation and/or ice crystal growth.”

Figure 6 caption: please specify that rows correspond to temperature, dRHi and w

Revised the figure caption: “ACI is examined for various ranges of temperature (in rows 1 and 4), dRHi (in rows 2 and 5), and d*w* (in rows 3 and 6).”

Figure 6: Make sure x-axes ranges are consistent with left most columns and the right most column

We modified the figures to make the axes range more comparable.

Line 343-345: You can test for this right? Compare it with Naer500.

We added a discussion when we first mentioned the nonlinearity in relation to Na_{100} in Section 3.3: “This nonlinearity with Na_{100} may suggest a nucleation mechanism shift from homogeneous freezing to heterogeneous freezing at higher Na_{100}. The higher Na_{100} may be associated with either higher concentrations of INPs or more effective INPs (or both), since a positive correlation between Na_{100} and Na_{500} was found (not shown). However, without direct INP measurements and aerosol composition measurements at the cirrus cloud levels in these former campaigns, one cannot rule out one possibility or the other.”

Figure 7 caption: think you labelled the red and green columns incorrectly

Thank you for catching this typo. It is reversed now.

Line 380-381: Careful, you're not getting information of cloud formation here. Should rephrase to "occurrence"

This is a good point. We corrected several locations by rephrasing them to cirrus cloud occurrence.

Line 453-455: It's difficult to visualize this. Perhaps provide some quantitative measure to confirm this?

We revised this sentence to discuss a more obvious improvement when using aerosols as predictors: "Adding aerosols as predictors shows larger differences in IWC values between the non-quiescent and vertically quiescent cirrus, which are also more similar to the observations compared with only using T+RHi+*w*. This result illustrates the effects of aerosols in addition to thermodynamic and dynamic effects.

Line 495-496: I'm unsure what this means. If this is indeed what you meant, source?

We can see that the previous text was not clear. We added a discussion when we first mentioned the nonlinearity in relation to Na_{100} in Section 3.3: "This nonlinearity with Na_{100} may suggest a nucleation mechanism shift from homogeneous freezing to heterogeneous freezing at higher Na_{100}. The higher Na_{100} may be associated either higher concentrations of INPs or more effective INPs (or both), since a positive correlation between Na_{100} and Na_{500} was found (not shown). However, without direct INP measurements and aerosol composition measurements at the cirrus cloud levels in these former campaigns, one cannot rule out one possibility or the other."

Line 506-507: Did you flip "necessary" and "sufficient"?

We can see why the previous description was confusing. We revised this paragraph in the discussion based on results of the revised Table 3 (i.e., after removing ATTREX, POSIDON, and START08), and this phrase about necessary or sufficient was removed.

Response to Reviewer 2's comments:

General Comments:

This is a very extensive observational study of cirrus clouds having near-global coverage, based on aircraft flights funded through NSF (7 campaigns) and NASA (5 campaigns). In particular, the smallest ice particles of the ice particle size distribution (PSD) are sampled, down to 1 µm, thus providing more useful information regarding the ice formation pathways (i.e., heterogeneous vs. homogeneous ice nucleation; henceforth het and hom). These ice PSD measurements are unique in that they have complementary measurements of relative humidity (RHi), aerosol particle PSDs, and vertical velocities (w). These complementary measurements are related to the ice PSD properties of ice water content (IWC), mean maximum dimension (Di), and number concentration (Ni) using a delta-delta method that correlates their fluctuations with those of the complementary measurements. Lastly, machine learning techniques are applied to better understand how IWC is affected by the complementary measurements.

I share the concerns expressed by Reviewer 1 regarding the practice of using in-cloud aerosol measurements since Na(500) (i.e., aerosol concentration between 0.5 µm and 1.0 µm) may be mostly small ice crystals. Why should fluctuations in Na(500) be so strongly correlated with fluctuations in IWC? What plausible physical process would explain these strong correlations? Using aerosol measurements just below cloud base could remedy this concern. Alternatively, if it could be shown that N_i(1-3µm) (i.e., the ice crystal number concentration between 1 and 3 microns as measured by the FCDP) is orders of magnitude less than Na(500), then it might be argued that ice crystals are a minor component of Na(500).

Our recent research shows that IWC and Ni track each other very closely when hom occurs. If Na for D > 0.5 µm here is strongly affected by Ni (as suggested by Reviewer 1), then these strong correlations may be partly due to fluctuations in hom (associated with higher IWC) correlated with fluctuations in Ni (associated with hom). Alternatively, one could argue that ISSRs (ice supersaturated regions) are common with higher INP (ice nucleating particle) concentrations impacting the RHi within these ISSRs to various degrees, resulting in correlations between IWC and Na(500) fluctuations. Such physical interpretations of these results are needed, even if they are only working hypotheses.

Thank you for this comment. Regarding examination of whether there are measurement artifacts that cause Na_{500} values to be correlated with ice microphysical properties, we took several steps to address them.

Regarding the comments of the correlations between Na_{500} and Ni, **Figure R1** below shows a time series of the NASA-DC3 campaign Research Flight (RF) 03, around UTC 25:40 to 26:00. Fluctuations of IWC are seen to be tightly correlated with Ni, as expected. However, the fluctuations of both Na_{100} and Na_{500} (last row) are found to be independent from those of IWC (first row). In fact, most of the in-cloud conditions are associated with Na_{500} values being zero. This indicates that the existence of ice particles is unlikely the cause of the higher Na_{500} values such as via small ice particle sublimation or large ice shattering. Because if that was the case, we would expect to see direct correlations between the fluctuations of the IWC and Na variables. Towards the end of this in-cloud period, Di decreases and Ni increases, but there are no measurements of Na_{500}. If there were to be a correlation between Na_{500} and small ice crystals, it should be when Di is smallest, which was not observed. In addition, since the existence of large aerosols ($Na_{500} > 0$) was observed less frequently compared with the existence of ice particles, this indicates that some of the ice particles are likely formed by homogeneous freezing. This also is consistent with the fact that ice nucleating particles (INPs) are very rare in the upper troposphere, and the existence of Na_{500} as a proxy of INP likely provides a significant support for ice nucleation by lowering the required energy barrier for heterogeneous freezing. We examined individual hourly segments of time series for all the campaigns used in this analysis. Here we only show one example, but no second-to-second correlation was found for other campaigns either.

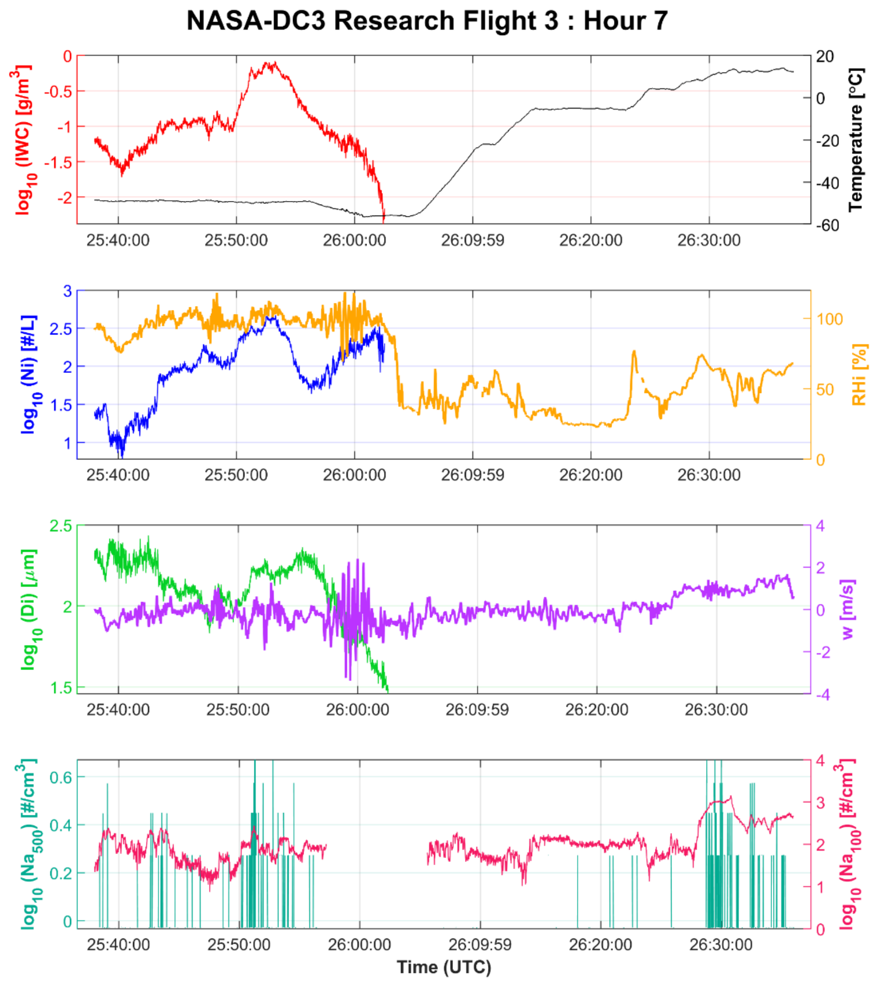

Figure R1. A case study of NASA DC-3 RF03 time series, illustrating the 1-Hz fluctuations of in-situ observations of ice microphysical properties (i.e., IWC, Ni and Di), aerosol number concentrations (Na_{100} and Na_{500}), and thermodynamic/dynamical variables (temperature, RHi, and w).

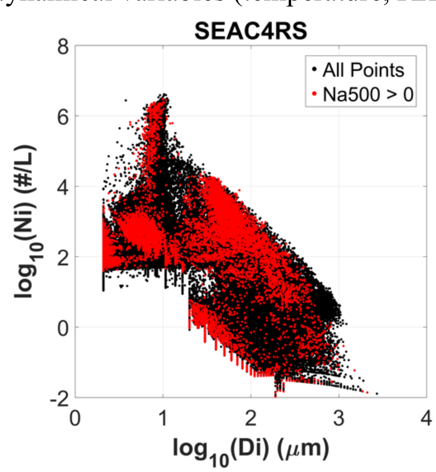

Figure R2. Correlations between Ni and Di in NASA SEAC[4]RS campaign, colored by the occurrences of Na_{500}. Black dots show all in-cloud samples (with or without Na_{500}), and red dots show in-cloud samples with $Na_{500} > 0$. All variables are plotted on a logarithmic scale.

Regarding the reviewer's comment about IWC and Ni track each other closely when homogeneous freezing occurs, we investigated whether there are correlations between occurrences of large aerosols and a certain size range of ice particles. **Figure R2** shows the distribution of ice crystal number concentrations (Ni) and mean diameters (Di), showing in-cloud samples with or without $Na_{500} > 0$. The samples with large aerosols occur at various Ni and Di ranges, not only concentrated at either smaller or larger ice particles. This result indicates that there is no evidence showing that sublimation of small ice or shattering of large ice could be the main cause of large aerosol occurrences measured.

Regarding the reviewer's comment on the possible correlations between Na_{500} and Ni of small ice (1-3 micron), we examined the time series of several campaigns and below is an example of NASA SEAC^{4}RS campaign RF03. The Ni (1-3 micron) is shown in the last row and is not directly correlated with Na_{500} in row 4 (**Figure R3**).

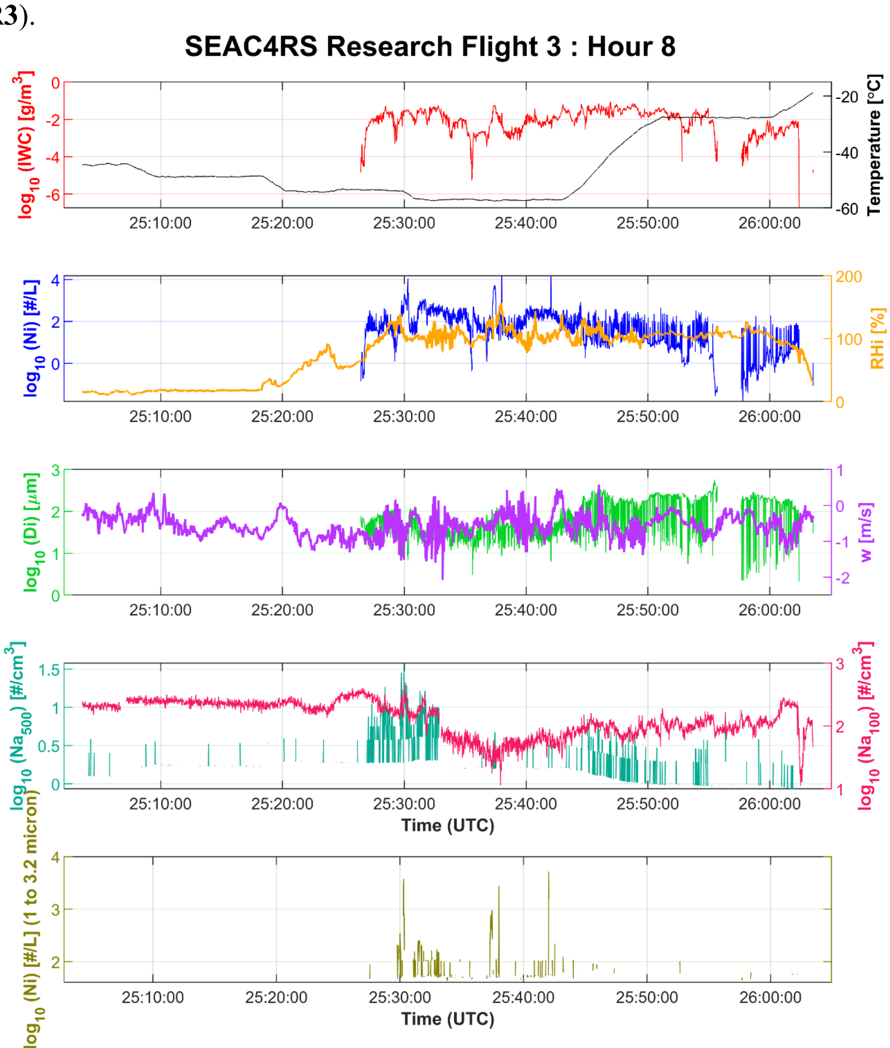

Figure R3. A case study of NASA SEAC^{4}RS RF03 time series, illustrating the 1-Hz fluctuations of in-situ observations of ice microphysical properties (i.e., IWC, Ni and Di), aerosol number concentrations (Na_{100} and Na_{500}), and thermodynamic/dynamical variables (temperature, RHi, and w). Ni for the small size range (1-3 micron) is shown in the last row.

Regarding the reviewer comment about whether ice supersaturated regions (ISSRs) are common with higher INP concentrations, we analyze whether large aerosol samples at in-cloud conditions are often associated with ISS conditions or not. The number of samples with $Na_{500} > 0$, $Na_{100} > 0$ for clear-sky or in-cloud conditions are counted separately for all RHi conditions (**Table R1**) and ice supersaturation (ISS) only **(Table R2**). Comparing the first columns in these two tables, only a small fraction (31 %) of the large aerosol samples at in-cloud conditions are associated with ISS. This result is likely caused by ice nucleation events happening before the sampling time stamp. Our previous study by Maciel et al. (2023) showed that the linear regression slope values are larger at nucleation phase and early growth phase, indicating stronger aerosol-cloud interactions (ACI) for those phases. The slopes decrease when cirrus clouds are in later growth and sedimentation phases, but it doesn't exclude the possibility that this positive correlation can still be seen after ice nucleation.

In addition, **Table R1** shows that only a small percentage of in-cloud conditions have large aerosols (~33%), while almost all in-cloud conditions have small aerosols. These results suggest that most of the in-cloud conditions may have already depleted the previously existing large aerosols by using them as INPs for ice nucleation, or these cirrus clouds are potentially formed by homogeneous freezing without Na_{500}. Another interesting feature we found by comparing these two tables is that the ratio of large aerosol number of samples associated with in-cloud versus clear-sky conditions significantly increases when ISSR is available compared with those seen at all RHi conditions.

Table R1. The number of 1-second samples of four conditions, including in- or out-of-clouds, with or without the existence of various types of aerosols (i.e., Na_{500} or Na_{100} values being greater than zero).

# of 1-s observations in each temperature range	In-cloud & $Na_{500} > 0$	In-cloud & $Na_{100} > 0$	Clear sky & $Na_{500} > 0$	Clear sky & $Na_{100} > 0$
$-50 < T \leq -40°C$	24026	90989	47658	374659
$-60 < T \leq -50°C$	26847	82362	40005	358825
$-70 < T \leq -60°C$	15755	27737	56543	167650
$-80 < T \leq -70°C$	61	3531	10010	24197

Table R2. Similar to Table R1, except for analyzing ice supersaturated conditions only.

# of 1-s observations in each temperature range	In-cloud & $Na_{500} > 0$ & RHi > 100 %	In-cloud & $Na_{100} > 0$ & RHi > 100 %	Clear sky & $Na_{500} > 0$ & RHi > 100 %	Clear sky & $Na_{100} > 0$ & RHi > 100 %
$-50 < T \leq -40°C$	8719	38587	1348	9848
$-60 < T \leq -50°C$	7286	29233	1152	7505
$-70 < T \leq -60°C$	4445	7603	332	2764
$-80 < T \leq -70°C$	16	682	1	273

We added this discussion to Section 3.3: "To further examine the role of aerosols in the ACI relationship, the number of samples of in-cloud and clear-sky conditions associated with large and small aerosols are analyzed. The results show that for large aerosol samples (i.e., $Na_{500} > 0$), 30 % of them are in-cloud while the rest are in clear-sky conditions. For small aerosol samples (i.e., $Na_{100} > 0$), 18 % of them are in-cloud. When restricted to ice supersaturated conditions only, a significant increase is seen for large aerosol samples associated with in-cloud conditions (75 %) while the rest were clear-sky conditions. Similarly, a significant increase is seen for small aerosol samples at in-cloud conditions (79 %) when ice supersaturation is available. In addition, when examining the distributions of Na_{500} at in-cloud conditions, the occurrences of large aerosols were seen at various Ni and Di ranges (not shown), suggesting that large aerosols were not solely observed when large or small ice crystals were available. These results suggest that it is more likely that the coexistence of aerosols and ice supersaturation leads to the formation of ice crystals instead of the other way around (i.e., occurrences of ice crystals affecting aerosol measurements)."

Regarding the reviewer's question about "*what plausible physical process would explain these strong correlations?*", we kept our original text that speculates Na_{500} serving as a proxy of INP concentrations at the cirrus level, after verifying that there is no second-to-second correlation between Na_{500} and ice microphysics. Our original text describing the potential role of large aerosols serving as INPs via heterogeneous freezing is copied here: "… larger aerosols produce stronger effects on cirrus (i.e., steeper slopes) than smaller aerosols shown by the slopes of linear regressions (Figure 6). In addition, near-linear correlations with positive slopes are seen between fluctuations of IWC, Ni, and Di relative to fluctuations of larger aerosols, while the correlations with smaller aerosols are nonlinear … This is likely because larger aerosols are more likely to freeze via the heterogeneous nucleation, while the smaller aerosols are more likely to freeze via homogeneous freezing." Our previous text also described the reason why direct measurements of INPs are very rare at cirrus level, and therefore Na_{500} is used as a proxy for INP concentrations: "Note that due to the limitations of former INP measurement techniques, that study focused on temperatures higher than -30 °C instead of the cirrus cloud regime (i.e., ≤ -40 °C). Other studies using the particle analysis by laser mass spectrometry (PALMS) instrument showed that particles with diameters > 500 nm are dominated by dust particles and nonvolatile sea-salt for number and mass concentrations (Murphy et al., 2019; Froyd et al., 2019). Both dust (e.g., Hoose and Möhler, 2012; Roesch et al., 2021) and sea salt (e.g., Patnaude et al., 2021b, 2024) have been previously reported to initiate heterogeneous freezing as INPs, which supports the speculation that Na_{500} may be used as a proxy for INP number concentrations."

We also conducted an analysis using clear-sky Na values calculated for every 100 seconds. The results are shown in Figures S6 and S7. **Figure S6** shows the correlations between the clear-sky $dlog_{10}Na$ values and $dlog_{10}IWC$. **Figure S7** shows the linear regressions between these two variables. Both figures show similar results compared with those shown in the main manuscript using in-cloud Na values. Discussion has been added to Section 3.5.

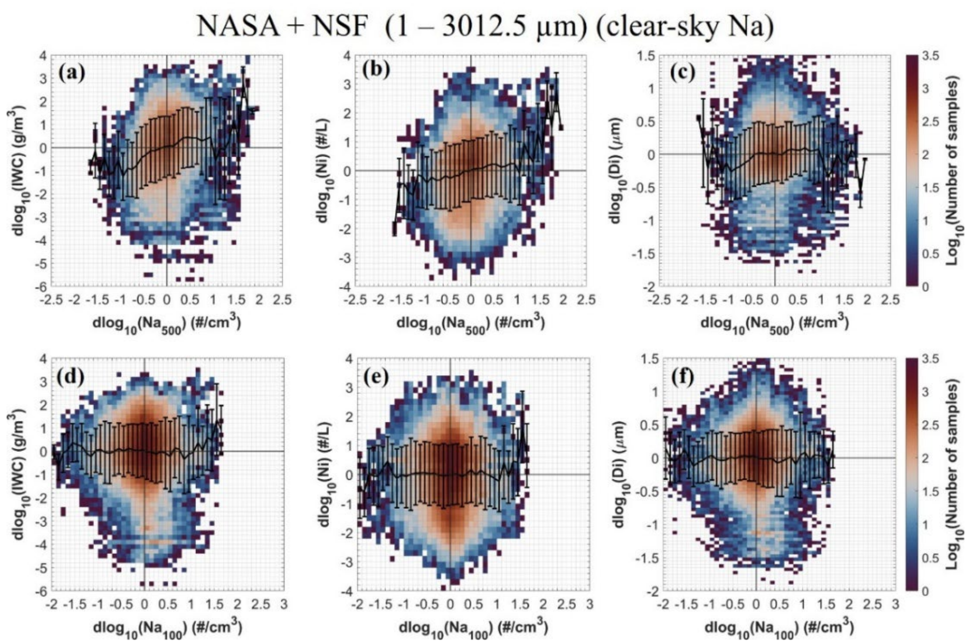

Figure S6. Similar to Figure 5, except for the analysis of clear-sky Na instead of in-cloud Na. Distributions of IWC, Ni, and Di with respect to (a-c) Na_{500} and (d-f) Na_{100} using the clear-sky Na values calculated at 100-s scale. Black lines and vertical bars denote the geometric means and standard deviations, respectively.

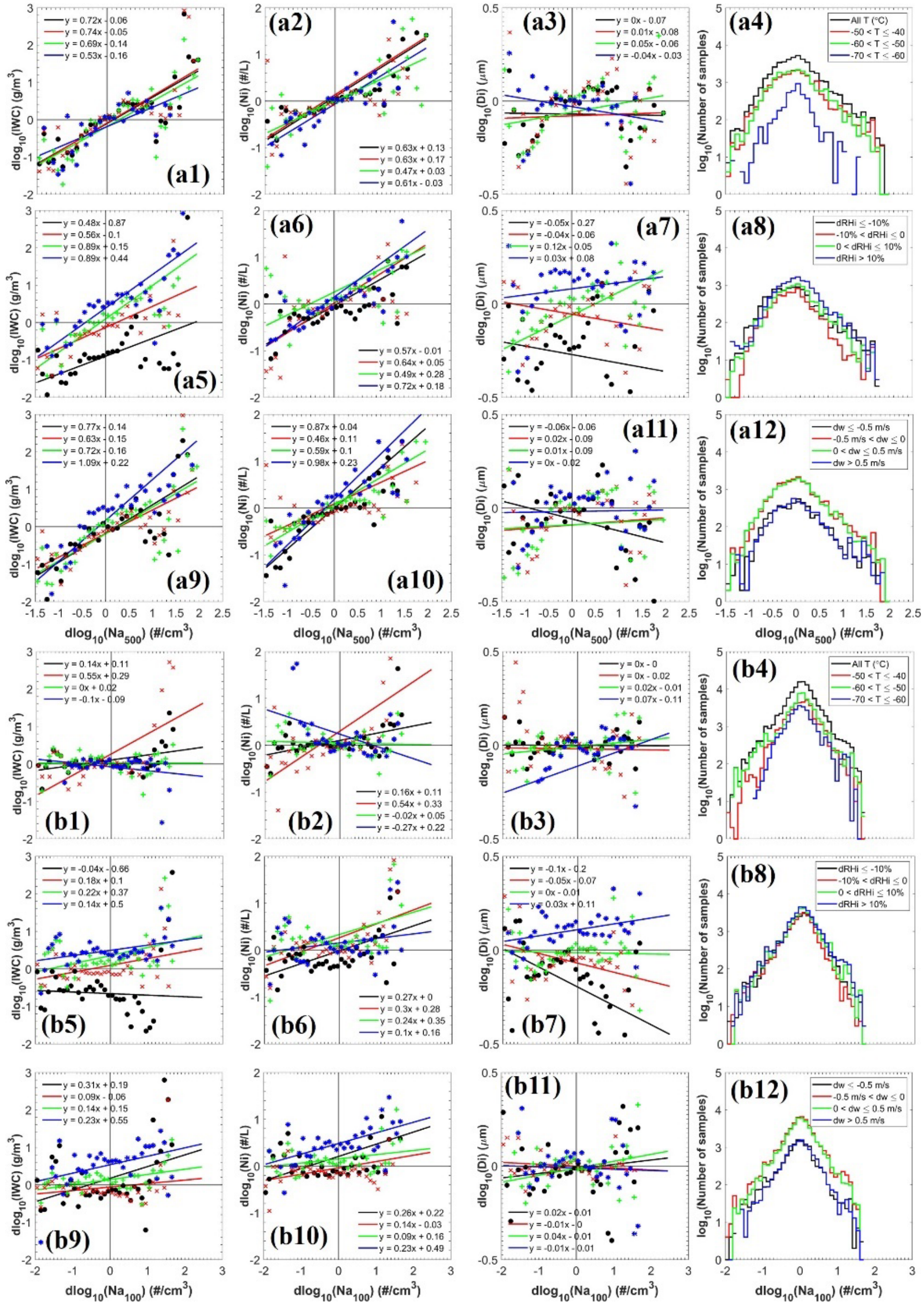

Figure S7. Similar to Figure 6 in the main manuscript, but using clear-sky Na values. ACI is examined for various ranges of temperature, dRHi, and d*w*. Colored dots represent geometric means of ice microphysical properties in each Na bin. Slope and intercept values are shown in the legend. The last column represents the number of samples.

Specific Comments:

1. Lines 25 – 26: I don't see the justification for this statement (cirrus coverage of 20% to 40%). Sassen et al. (2009) estimates that global coverage for cirrus is 17%, while in Mace and Wrenn (2013), I could not find any mention of coverage.

We thank the reviewer for catching this issue. We revised the references in this sentence: "The global cirrus coverage was reported to range from 10 % to 30 % from the polar regions to the tropics, respectively, based on observations of the Cloud-Aerosol Lidar and Infrared Pathfinder Satellite Observations (CALIPSO) satellite (Sassen et al., 2008 in their Figure 2). Wang et al. (2024) showed cirrus frequency around 20 % – 25 % at various latitudes and longitudes (in their Figure S6) based on several satellite products (e.g., CALIPSO and CloudSat) … For instance, the cirrus frequencies derived from satellite data may be underestimated since many cirrus clouds were reported to have thin optical thickness (less than 0.3) that may be too tenuous to be effectively captured by satellites (Sassen and Campbell, 2001)."

2. Lines 48 – 50: Please support this statement with a reference. Cziczo et al. 2013 seems appropriate.

Thanks for catching the missing reference. We added it.

3. Line 107: Jensen et al. 2017b is cited for POSIDON but POSIDON is never mentioned in that article, which is concerned only with ATTREX. A good POSIDON reference is Schoeberl et al. (2019, JGR).

Thank you for the suggestion. We moved the Jensen et al. (2017b) to part of the ATTREX citation and added Schoeberl et al. (2019) to POSIDON's citation.

Reference added:
Schoeberl, M. R., Jensen, E. J., Pfister, L., Ueyama, R., Wang, T., Selkirk, H., et al.: Water vapor, clouds, and saturation in the tropical tropopause layer. Journal of Geophysical Research: Atmospheres, 124, 3984–4003, https://doi.org/10.1029/2018JD029849, 2019.

4. Lines 129 – 131: These PSD properties are defined in the abstract but not the text. Is that consistent with ACP policy? Also, Di is defined as number-weighted mean diameter, but diameter applies only to spheres. Please provide a more accurate definition, such as mean maximum dimension.

We revised this part to add definitions of these terminologies and explanations of Di: "The ice microphysical properties to be examined include ice water content (IWC), ice crystal number concentration (Ni), and number-weighted mean diameter (Di). Here Di is calculated based on the maximum dimension of the ice particle."

5. Lines 171 – 182: Regarding the NSF data, the Fast-2DC has a physical measurement range from 62.5 um to 1600 um, with 25 um bin widths (as stated here). Throwing out the first 3 bins would then limit the sampling range to 137.5 um to 1600 um. The measurement range of the CDP is from 1 to 50 um. This leaves a 87.5 um gap between 50 and 137.5 um. How is this gap addressed?

Thank you for pointing this out. We can see that our previous description caused some misunderstanding. The first 3 bins of the Fast-2DC probe were already thrown out in the archived NSF datasets, i.e., the size range of Fast-2DC starts from 62.5 µm and ends at 3200 µm.

We did not throw any more small ice crystals after the first three bins were removed. Eventually, the Fast-2DC probe (62.5 – 3200 µm) was combined with the CDP probe (2 – 50 µm). Note that a small gap at 50 – 62.5 µm does exist, and we quantified the impact of this gap based on ice particle size distributions (PSDs) from a global climate model simulation output. Here we use model simulations to conduct this test because the cloud probes cannot provide 0 – infinity in size range. After testing PSD of simulations from a global climate model, this size gap contributes to 4 % of IWC and 0.8 % of Ni relative to their values at 2 – 3200 µm. Because this size gap has a relatively small impact and the interpolation process may introduce other uncertainties, we did not attempt to fill in this small size gap through interpolation.

We added clarification in this section: "For the Fast-2DC probe, the first 3 bins were already discarded in the archived data to minimize uncertainties, i.e., starting the particle size distributions (PSDs) at 62.5 µm, and the last few bins (> 3012.5 µm) were further discarded to reach a similar size range as the 2DS probe. After these procedures, the measurements of these probes were combined. That is, in the NSF campaigns, the CDP probe measurements at 2 – 50 µm were combined with the Fast-2DC probe measurements at 62.5 – 3012.5 µm, providing a final size range of 2 – 3012.5 µm. To quantify the impact of the remaining size gap (50 – 62.5 µm) of the merged NSF data, IWC and Ni of this size gap were calculated based on ice crystal PSDs from global climate model simulations of the NCAR CESM2 / CAM6. The results show that the size gap of 50 – 62.5 µm accounts for 4 % of IWC and 0.8 % of Ni relative to their values at 2 – 3200 µm, respectively. Thus, we did not attempt to interpolate the data to fill this small size gap to avoid introducing more uncertainties through the interpolation assumptions."

6. Line 247 – 250: At the bottom of Sect. 5.1.1 in Kramer et al. (2020) is the statement: "Because of the dangerous nature of measurements under such conditions, the frequency of convective – and also orographic wave cirrus – is underrepresented in the entire in situ climatology." Could this be an issue in this dataset as well? Moreover, in Sect. 4.2.2 of this article, we find "the higher (Ni) values at warmer temperatures in the Krämer et al. (2009) data set (Fig. S6, Supplement) were caused by flights where lee wave cirrus behind the Norwegian mountains were probed". To summarize, higher Ni values are associated with orographic gravity wave (OGW) cirrus clouds, and OGW cirrus are characterized by higher updrafts, more conducive to hom. In the satellite remote sensing studies of Gryspeerdt et al. (2018) and Mitchell et al. (2018), there are large regions of elevated Ni over and downwind of mountain barriers. Figure 1 of this paper does not show much sampling of such regions. Is it fair to say that OGW cirrus may have been under-sampled in these datasets leading to an underestimation of hom in the midlatitudes and polar regions? If so, please indicate this in the article.

We thank the reviewer for pointing out that these sampling biases may cause the under-representation of certain types of cirrus clouds in this dataset. We added a paragraph to discuss the caveat after we discussed the regional differences at the end of Section 3.1: "Caution should be paid regarding the sampling domains of the field campaigns used in this analysis. Because the aircraft platforms used in these campaigns were not safe for storm penetration or sampling of highly convective conditions, cirrus clouds near the convective core are expected to be under-represented. This under-representation of convective cirrus by aircraft observations was also pointed out by Krämer et al. (2020). In addition, previous studies showed that the higher Ni values were often associated with orographic gravity wave (OGW) cirrus clouds, especially over and downwind of mountain barriers, as seen in aircraft (Krämer et al., 2009) and satellite observations (e.g., Gryspeerdt et al., 2018; Mitchell et al., 2018). Flight maps in this study (Figure 1) show limited sampling of such regions, suggesting that the OGW cirrus may be under-sampled. As a result of the under-sampling of convective and OGW cirrus, the impacts of homogeneous freezing may be underestimated, since higher updrafts in these types of cirrus conditions are conducive to higher cooling rates, higher ice supersaturation, and higher frequencies of homogeneous freezing."

The references mentioned above are:

Gryspeerdt, E., Sourdeval, O., Quaas, J., Delanoë, J., Krämer, M., and Kühne, P.: Ice crystal number concentration estimates from lidar–radar satellite remote sensing – Part 2: Controls on the ice crystal number concentration, Atmos. Chem. Phys., 18, 14351–14370, https://doi.org/10.5194/acp-18-14351-2018, 2018.

Krämer, M., Schiller, C., Afchine, A., Bauer, R., Gensch, I., Mangold, A., Schlicht, S., Spelten, N., Sitnikov, N., Borrmann, S., de Reus, M., and Spichtinger, P.: Ice supersaturations and cirrus cloud crystal numbers, Atmos. Chem. Phys., 9, 3505–3522, https://doi.org/10.5194/acp-9-3505-2009, 2009.

Mitchell, D. L., Garnier, A., Pelon, J., and Erfani, E.: CALIPSO (IIR–CALIOP) retrievals of cirrus cloud ice-particle concentrations, Atmos. Chem. Phys., 18, 17325–17354, https://doi.org/10.5194/acp-18-17325-2018, 2018.

7. Lines 272-275: Perhaps it is worth mentioning that the NSF data exhibits median Ni values near log(1.5), or 32 L-1, which is similar to median Ni in Kramer et al. (2020).

We added the discussion: "The NSF dataset exhibits median Ni values near $10^{1.5}$ L^{-1}, or 32 L^{-1}, which is similar to the median Ni in Krämer et al. (2020)."

8. Lines 436 – 441: After studying Table 3, the "take-home message" for me is the following: At scales of 50-s or greater, dT + dRHi appears to be the most influential IWC predictor for quiescent cirrus. The 250-s scale appears to be the best IWC predictor for non-quiescent cirrus (regarding dT + dRHi), with dlogNa(500) also having an impact in addition to dT + dRHi. Should something along these lines be stated here?

The new Table 3 has been updated to remove ATTREX, POSIDON, and START08 campaigns from all predictions. Thus, the values slightly changed. This main feature mentioned by the review still exists and was added to the text: "Using dT+dRHi as predictors, the accuracies of predicting the sign of $d\log_{10}$IWC for vertically quiescent cirrus are 64.04 %, 70.34 %, 69.44 %, and 71.74 % for 1-s, 50-s, 250-s, and 500-s averaged observations, respectively, indicating the dT+dRHi predictors from 50-s to 500-s scales are more influential on the IWC prediction in vertically quiescent cirrus… On the other hand, examining the non-quiescent cirrus, even though the dT+dRHi prediction provides the highest accuracy of 80.14 % by using 250-s averaged observations, the 500-s averaged observations provide the lowest accuracy of 66.14 % among all spatial scales, indicating a sudden decrease in the impacts of RHi conditions around 100 km surrounding non-quiescent cirrus."

9. Lines 444 – 448: For quiescent cirrus, it is true that IWC peaks ~ 110% RHi, but for non-quiescent cirrus, IWC peaks for RHi > 150%. Please consider mentioning this important finding.

We thank the reviewer for pointing out this unique feature. We added this description: "… (2) two peaks of IWC values, one at small ice supersaturation (i.e., RHi of 110 %) which is more pronounced for quiescent cirrus, and the other one at high ice supersaturation (RHi of 150 % – 160 %) which is more pronounced for non-quiescent cirrus, …"

10. Lines 455 – 459: In Fig. 10, what is responsible for the differences between panels a-b-c in the 1st row and panels d-e-f in the 2nd row?

We added text inside the revised **Figure 10** (below), on the left-hand side of each row to indicate the ML predictors being used. We also added two more rows using the predictors T+RHi+*w*+Na_{500}+Na_{100}. The differences between each row are caused by different sets of predictors. Adding RHi and *w* significantly reduces the biases of IWC magnitudes, while adding aerosol information reduces the biases even further, especially for low temperatures, small ice supersaturation, and strong updrafts/downdrafts.

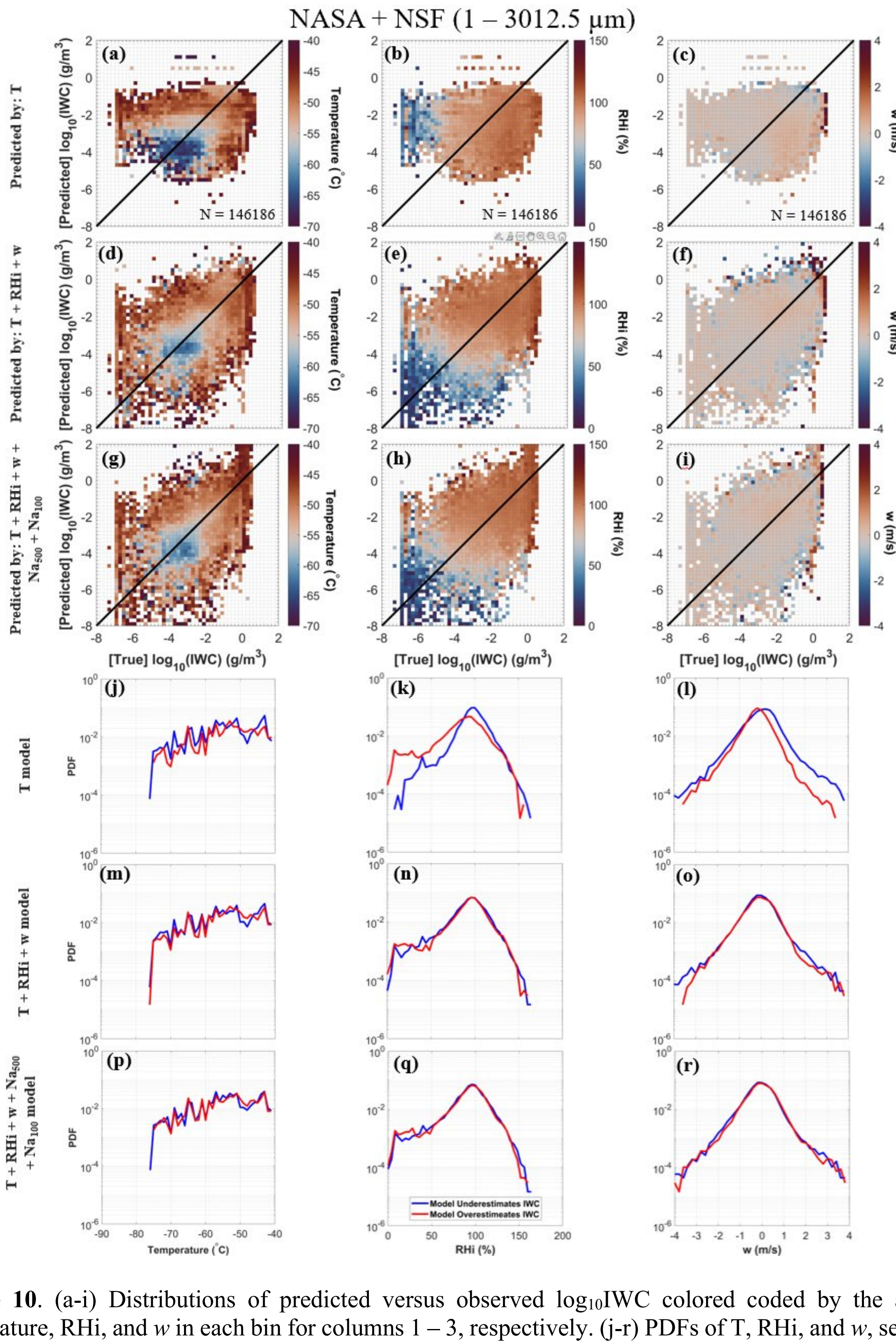

Figure 10. (a-i) Distributions of predicted versus observed $\log_{10}$IWC colored coded by the average temperature, RHi, and *w* in each bin for columns 1 – 3, respectively. (j-r) PDFs of T, RHi, and *w*, separated by when IWC is underestimated or overestimated by the ML model. Rows 1 and 4 are predicted by T only. Rows 2 and 5 are predicted by T+RHi+*w*. Rows 3 and 6 are predicted by T+RHi+*w*+Na_{500}+Na_{100}.

11. Lines 513 -514: For a broader perspective, please mention the cirrus climatology of Kramer et al. (2020) and the number of field campaigns employed and their latitudes, surface types (land vs. ocean), and other relevant factors.

We rewrote this paragraph to consider the dataset from Krämer et al. (2020) as well as the overall geographical coverage of both studies: "The compiled in-situ observational dataset of cirrus clouds in this study provided a complementary dataset in terms of geographical coverage to the previous study of Krämer et al. (2020). That study analysed cirrus cloud observations from 24 field campaigns, including 5 campaigns that were also used in this study, i.e., START08, CONTRAST, MACPEX, ATTREX-2014, and POSIDON. That study showed more samples over Europe, Africa, Australia, and South America compared with this study. When assessing the geographical coverage of both studies, we identified several regions with fewer samples – (a) the polar regions in both hemispheres, (b) the Northern Hemisphere midlatitudes over ocean, and (c) the Southern Hemisphere midlatitudes over both ocean and land."

12. Lines 514 – 516: As mentioned, the properties of orographic gravity wave (OGW) cirrus may differ considerably from other cirrus clouds and be widespread in coverage as noted in Joos et al. (2008, JGR), Barahona et al. (2017, Nature), Kramer et al. (2020, ACP), Mitchell et al. (2018, ACP), Gryspeerdt et al. (2018, ACP), Lyu et al. (2023, JGR) and other studies. In Kramer et al. (2020), it was stated that OGW cirrus clouds were under-sampled due to dangerous flight conditions resulting from the higher updrafts. The same is likely true of this study. Please mention here this need to sample OGW cirrus clouds.

We added more discussions on different cirrus types: "In addition, both studies had fewer samples over mountainous regions conducive to OGW cirrus, which may not cover the entire distributions of cloud properties. Previously, considerably different ice microphysical properties and widespread coverage were found in OGW cirrus (e.g., Joos et al., 2008; Barahona et al., 2017; Mitchell et al., 2018; Gryspeerdt et al., 2018; Krämer et al., 2020; Lyu et al., 2023). Last but not the least, the majority of the field campaigns used in both studies (e.g., U.S. NSF campaigns) captured cirrus clouds as targets of opportunity instead of sampling them as the main scientific objective. Thus, more purposely designed comparative studies among cirrus clouds formed under various synoptic dynamical conditions (i.e., convective, orographic, and in-situ cirrus) are also still warranted."

New references added to the manuscript:

Barahona, D., Molod, A. and Kalesse, H.: Direct estimation of the global distribution of vertical velocity within cirrus clouds. Sci Rep 7, 6840, https://doi.org/10.1038/s41598-017-07038-6, 2017.

Gryspeerdt, E., Sourdeval, O., Quaas, J., Delanoë, J., Krämer, M., and Kühne, P.: Ice crystal number concentration estimates from lidar–radar satellite remote sensing – Part 2: Controls on the ice crystal number concentration, Atmos. Chem. Phys., 18, 14351–14370, https://doi.org/10.5194/acp-18-14351-2018, 2018.

Joos, H., Spichtinger, P., Lohmann, U., Gayet, J.-F., and Minikin, A.: Orographic cirrus in the global climate model ECHAM5, J. Geophys. Res., 113, D18205, doi:10.1029/2007JD009605, 2008.

Lyu, K., Liu, X., Bacmeister, J., Zhao, X., Lin, L., Shi, Y., & Sourdeval, O.: Orographic cirrus and its radiative forcing in NCAR CAM6. Journal of Geophysical Research: Atmospheres, 128, e2022JD038164. https://doi.org/10.1029/2022JD038164, 2023.

Technical Comments:

1. Lines 159 – 161: The FCAS, being an aerosol probe, must have a measurement range of 70 - 1000 nm, not microns.

We thank the reviewer for catching the typo. It is revised to nm.

2. Line 433: Possible typo: 50 km => 250 km?

We revised this sentence: "… the 500-s averaged observations provide the lowest accuracy of 66.14 % among all spatial scales, indicating a sudden decrease in the impacts of RHi conditions around 100 km surrounding non-quiescent cirrus."